Inorganic Chemistry

Article

pubs.acs.org/IC

Neutral Six-Coordinate and Cationic Five-Coordinate Silicon(IV) Complexes with Two Bidentate Monoanionic *N,S*-Pyridine-2-thiolato(−) Ligands

Johannes A. Baus,[†] Christian Burschka,[†] Rüdiger Bertermann,[†] Célia Fonseca Guerra,[‡] F. Matthias Bickelhaupt,*[,‡,§] and Reinhold Tacke*[,†]

[†]Institut für Anorganische Chemie, Universität Würzburg, Am Hubland, 97074 Würzburg, Germany

[‡]Department of Theoretical Chemistry, Amsterdam Center for Multiscale Modeling (ACMM), VU University Amsterdam, De Boelelaan 1083, 1081 HV Amsterdam, The Netherlands

[§]Institute of Molecules and Materials, Radboud University Nijmegen, Heyendaalseweg 135, 6525 AJ Nijmegen, The Netherlands

Supporting Information

ABSTRACT: A series of neutral six-coordinate silicon(IV) complexes (**4**−**11**) with two bidentate monoanionic *N,S*-pyridine-2-thiolato ligands and two monodentate ligands R^1 and R^2 was synthesized (**4**, $R^1 = R^2 = Cl$; **5**, $R^1 = Ph$, $R^2 = Cl$; **6**, $R^1 = Ph$, $R^2 = F$; **7**, $R^1 = Ph$, $R^2 = Br$; **8**, $R^1 = Ph$, $R^2 = N_3$; **9**, $R^1 = Ph$, $R^2 = NCO$; **10**, $R^1 = Ph$, $R^2 = NCS$; **11**, $R^1 = Me$, $R^2 = Cl$). In addition, the related ionic compound **12** was synthesized, which contains a cationic five-coordinate silicon(IV) complex with two bidentate monoanionic *N,S*-pyridine-2-thiolato ligands and one phenyl group (counterion: I^-). Compounds **4**−**12** were characterized by elemental analyses, NMR spectroscopic studies in the solid state and in solution, and crystal structure analyses (except **7**). These structural investigations were performed with a special emphasis on the sophisticated stereochemistry of these compounds. These experimental investigations were complemented by computational studies, including bonding analyses based on relativistic density functional theory.

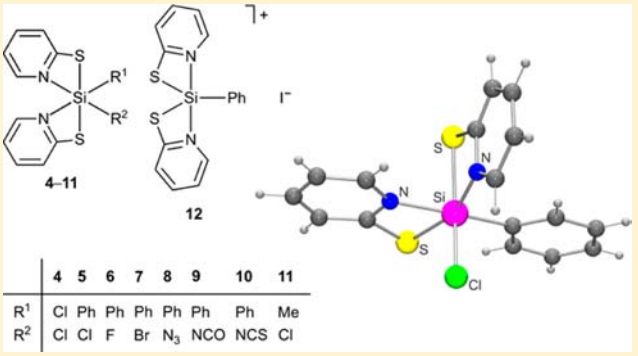

INTRODUCTION

Neutral six-coordinate bis[amidinato(−)]silicon(IV) complexes with their two highly strained four-membered SiNCN chelate rings (N−Si−N, 68−70°), such as **1**−**3**, are thermodynamically stable compounds.[1] This finding prompted us to investigate the synthetic potential of the *N,S*-pyridine-2-thiolato(−) ligand in the chemistry of higher-coordinate silicon. Coordination of this particular monoanionic ligand to silicon in a bidentate fashion would also result in the formation of a strained four-membered SiSCN chelate ring [for higher-coordinate silicon(IV) complexes with sulfur and/or pyridine-nitrogen ligand atoms, see refs 2 and 3]. In the coordination chemistry of transition metals, the *N,S*-pyridine-2-thiolato(−) ligand is well established,[4] but far fewer examples are reported in main-group chemistry,[5−8] with most examples being described for tin(IV).[7] Quite surprisingly, silicon(IV) complexes with this N,S-ligand have not yet been reported. We have now succeeded in synthesizing compounds **4**−**11**, the first six-coordinate silicon(IV) complexes with bidentate *N,S*-pyridine-2-thiolato(−) ligands, and the related ionic compound **12**, the first five-coordinate silicon(IV) complex with *N,S*-pyridine-2-thiolato(−) ligands (Scheme 1; for selected reviews on higher-coordinate silicon compounds, see ref 9). We report here on the synthesis of compounds **4**−**12**, their NMR spectroscopic characterization in the solid state and in solution, and their structural characterization by single-crystal X-ray diffraction (except **7**). The structural characterization of **4**−**12** was performed with a special emphasis on the sophisticated stereochemistry of these compounds (potential existence of diastereoisomers). These experimental investigations were complemented by computational studies, which provide information on the structure and relative stabilities as well as the bonding mechanism behind the observed and computed trends of these silicon(IV) complexes.

RESULTS AND DISCUSSION

Syntheses. Compounds **4**, **5**, and **11** were synthesized according to Scheme 2 by treatment of the corresponding chlorosilanes (**4**, $SiCl_4$; **5**, $PhSiCl_3$; **11**, $MeSiCl_3$) with 2 mol equiv each of 2-pyridinethiol and triethylamine in tetrahydrofuran (yields: **4**, 90%; **5**, 98%; **11**, 98%). Compounds **6**−**10** were prepared according to Scheme 3, starting from the corresponding chlorosilicon(IV) complex **5**. The fluorosilicon-

Received: July 4, 2013
Published: September 6, 2013

   dx.doi.org/10.1021/ic401698a | Inorg. Chem. 2013, 52, 10664−10676

Scheme 1. Chemical Structures of the Six-Coordinate Silicon(IV) Complexes 1−11 and the Five-Coordinate Silicon(IV) Complex 12

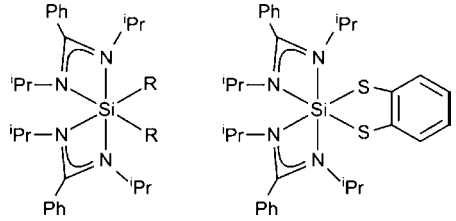

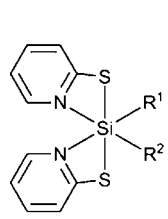

	R^1	R^2
4	Cl	Cl
5	Ph	Cl
6	Ph	F
7	Ph	Br
8	Ph	N_3
9	Ph	NCO
10	Ph	NCS
11	Me	Cl

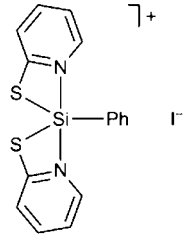

Scheme 2. Syntheses of Compounds 4, 5, and 11

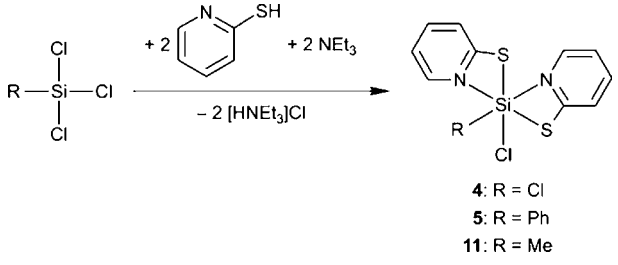

Scheme 3. Syntheses of Compounds 6−10

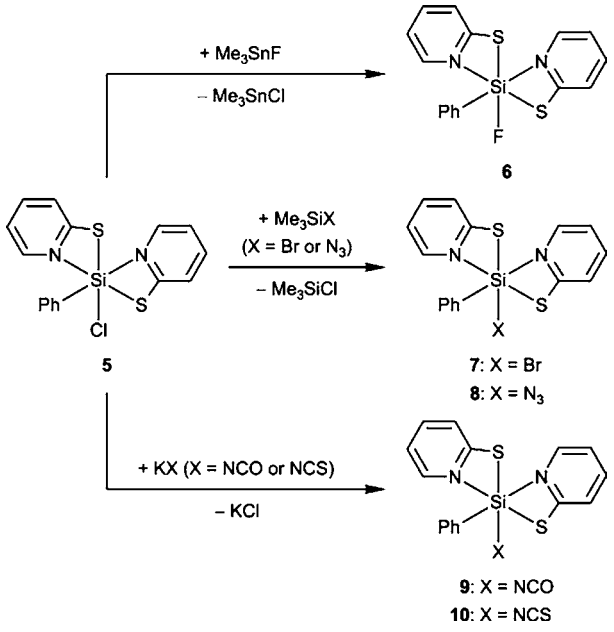

Scheme 4. Synthesis of Compound 12

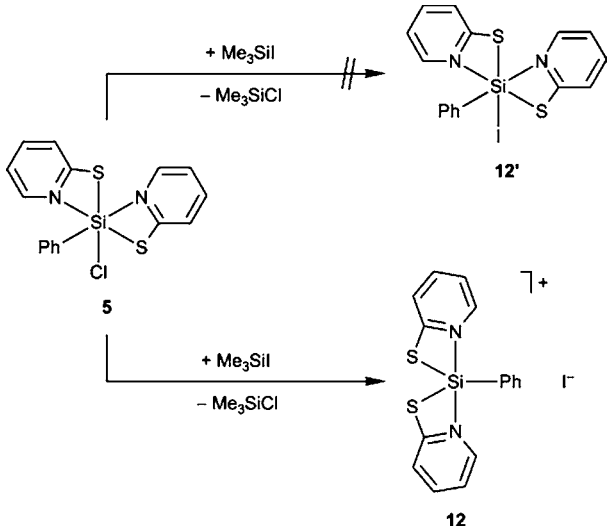

(IV) complex **6** was obtained by the reaction of **5** with 1 mol equiv of fluorotrimethylstannane in tetrahydrofuran (yield 84%). The bromosilicon(IV) complex **7** was synthesized by the treatment of **5** with an excess of bromotrimethylsilane (yield 68%), and the azidosilicon(IV) complex **8** was obtained by the reaction of **5** with 1 mol equiv of azidotrimethylsilane (yield 76%). Both syntheses were performed in acetonitrile. The synthetic method used for the preparation of **7** and **8** could not be applied to the syntheses of the analogous (cyanato-*N*)silicon(IV) complex **9** and (thiocyanato-*N*)silicon(IV) complex **10**. Instead, compounds **9** and **10** were prepared by the treatment of **5** with 1.1 mol equiv of potassium cyanate and potassium thiocyanate, respectively, in acetonitrile (yields: **9**, 88%; **10**, 83%). Quite interestingly, the treatment of **5** with iodotrimethylsilane in acetonitrile did not yield the expected neutral six-coordinate silicon complex **12′**; instead, the ionic compound **12** was isolated, which contains a cationic five-coordiante silicon(IV) complex (Scheme 4; yield 66%). Compounds **4**−**12** were isolated after crystallization from acetonitrile as highly moisture-sensitive crystalline solids. Their identities were established by elemental analyses (C, H, N, and S), NMR spectroscopic studies in the solid state (^{15}N, ^{19}F, and ^{29}Si) and in solution (^{1}H, ^{13}C, ^{19}F, and ^{29}Si), and crystal structure analyses (except **7**).

Crystal Structure Analyses. Compounds **4**−**6** and **8**−**12** were structurally characterized by single-crystal X-ray diffraction. All attempts to grow suitable single crystals for a crystal structure analysis of **7** failed. The crystal data and experimental parameters used for the crystal structure analyses **4**−**6** and **8**−**12** are given in the Supporting Information (Tables S1 and S2). The molecular structures of **4**−**6** and **8**−**11** are depicted in Figures 1−8, and the structure of the cation of **12** is shown in Figure 9. Selected bond lengths and angles are given in the respective captions.

dx.doi.org/10.1021/ic401698a | *Inorg. Chem.* 2013, 52, 10664−10676

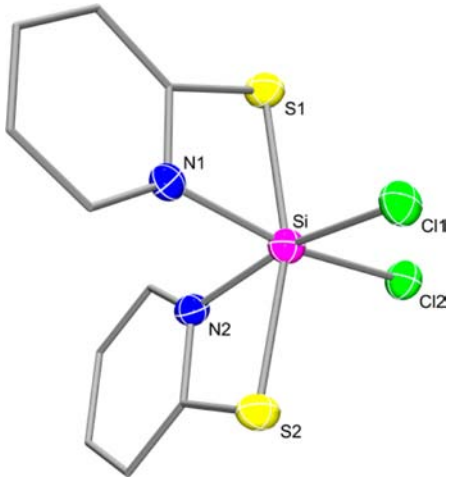

Figure 1. Molecular structure of **4** in the crystal (probability level of displacement ellipsoids 50%). Selected bond lengths (Å) and angles (deg): Si–Cl1 2.1648(15), Si–Cl2 2.1897(16), Si–S1 2.2649(13), Si–S2 2.2697(13), Si–N1 1.949(3), Si–N2 1.949(3); Cl1–Si–Cl2 93.69(6), Cl1–Si–S1 97.73(6), Cl1–Si–S2 93.49(6), Cl1–Si–N1 91.56(10), Cl1–Si–N2 166.01(10), Cl2–Si–S1 92.84(6), Cl2–Si–S2 98.77(6), Cl2–Si–N1 165.21(10), Cl2–Si–N2 89.44(10), S1–Si–S2 163.29(6), S1–Si–N1 72.74(10), S1–Si–N2 95.72(10), S2–Si–N1 94.69(10), S2–Si–N2 72.55(9), N1–Si–N2 88.79(13).

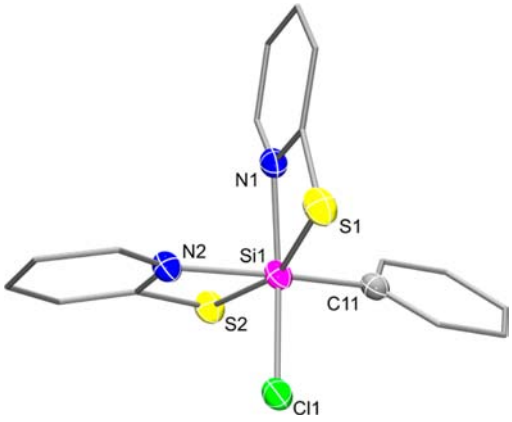

Figure 2. Molecular structure of diastereomer **5a** in the crystal of **5** (probability level of displacement ellipsoids 50%). Selected bond lengths (Å) and angles (deg): Si1–Cl1 2.2263(12), Si1–S1 2.3049(13), Si1–S2 2.2980(13), Si1–N1 1.973(3), Si1–N2 1.954(3), Si1–C11 1.906(3); Cl1–Si1–S1 93.90(4), Cl1–Si1–S2 97.18(5), Cl1–Si1–N1 164.07(7), Cl1–Si1–N2 87.06(8), Cl1–Si1–C11 96.15(10), S1–Si1–S2 160.69(5), S1–Si1–N1 72.04(8), S1–Si1–N2 92.96(8), S1–Si1–C11 98.69(9), S2–Si1–N1 94.46(8), S2–Si1–N2 71.95(7), S2–Si1–C11 95.79(9), N1–Si1–N2 86.25(11), N1–Si1–C11 93.44(12), N2–Si1–C11 167.65(11).

The silicon-coordination polyhedra of **4**–**6** and **8**–**11** are strongly distorted octahedra, with maximum deviations from the ideal 90° and 180° angles ranging from 17.45(9)° to 20.05(9)° and from 16.71(6)° to 22.45(8)°, respectively. All of the structures discussed herein have two chelating monoanionic *N*,*S*-pyridine-2-thiolato ligands in common, which, together with the silicon-coordination center, build up two highly strained four-membered SiSCN chelate rings, with S–Si–N bite angles ranging from 69.95(9)° to 72.55(9)°. As can be seen from Scheme 5, there are four possible assemblies of these bidentate ligands (diastereomers **A**–**D**), and two of them are observed in the crystal of **5** [cocrystallization of the

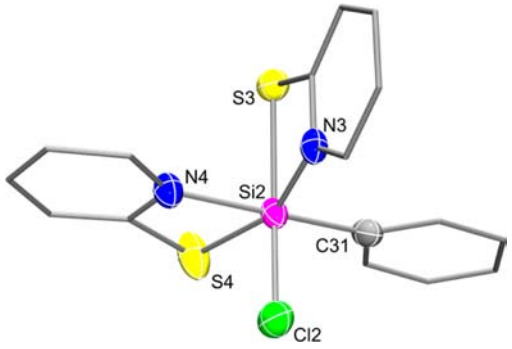

Figure 3. Molecular structure of diastereomer **5b** in the crystal of **5** (occupation factor 87%; probability level of displacement ellipsoids 50%). Selected bond lengths (Å) and angles (deg): Si2–Cl2 2.1924(16), Si2–S3 2.4167(16), Si2–S4 2.3006(17), Si2–N3 1.893(3), Si2–N4 1.948(3), Si2–C31 1.913(3); Cl2–Si2–S3 163.60(8), Cl2–Si2–S4 97.80(7), Cl2–Si2–N3 93.58(14), Cl2–Si2–N4 90.36(10), Cl2–Si2–C31 96.27(11), S3–Si2–S4 94.91(6), S3–Si2–N3 71.09(13), S3–Si2–N4 84.01(9), S3–Si2–C31 91.70(11), S4–Si2–N3 157.78(13), S4–Si2–N4 71.02(9), S4–Si2–C31 99.84(13), N3–Si2–N4 89.96(15), N3–Si2–C31 97.80(17), N4–Si2–C31 169.43(16). The structure of **5b** is disordered (interchanged positions of Cl2 and S3) with a second molecule (occupation factor 13%) that represents the antipode of the enantiomer depicted above. The molecular structures of the two enantiomers are very similar.

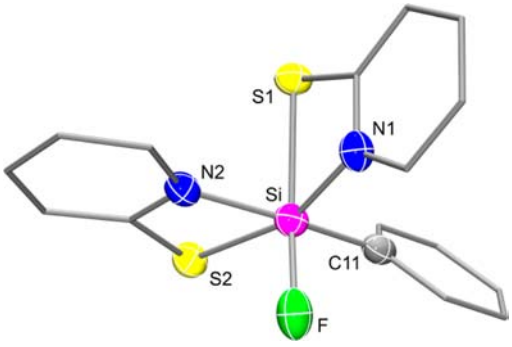

Figure 4. Molecular structure of **6** in the crystal (probability level of displacement ellipsoids 50%). Selected bond lengths (Å) and angles (deg): Si–S1 2.4452(11), Si–S2 2.3192(10), Si–F 1.798(2), Si–N1 1.903(2), Si–N2 1.950(3), Si–C11 1.911(4); S1–Si–S2 95.04(4), S1–Si–F 162.67(8), S2–Si–F 98.39(7), S1–Si–N1 69.95(9), S1–Si–N2 84.49(8), S1–Si–C11 92.32(10), S2–Si–N1 160.34(8), S2–Si–N2 71.65(8), S2–Si–C11 96.65(9), F–Si–N1 94.36(11), F–Si–N2 89.39(10), F–Si–C11 96.92(11), N1–Si–N2 93.69(11), N1–Si–C11 96.59(12), N2–Si–C11 167.48(12).

diastereomers **5a** (**A**) and **5b** (**C**); molar ratio 1:1]. In the case of compounds **4**, **6**, and **8**–**11**, only one of the four possible diastereomers is found (**4**, diastereomer **A**; **6** and **8**–**11**, diastereomer **C**). The positions of the two sulfur ligand atoms relative to each other make the main difference between the two structures observed. In the case of compounds **4** and **5a**, the sulfur atoms are in trans positions with S–Si–S angles of 163.29(6)° and 160.69(5)°, respectively. The sulfur atoms in **5b**, **6**, and **8**–**11** occupy cis positions [S–Si–S angles, 92.10(4)° to 95.04(4)°], and one of the two sulfur atoms and the (pseudo)halogeno ligand are in trans positions [S–Si–R angles (R = Cl, F, N_3, NCO, NCS), 161.08(9)–163.57(8)°]. In the latter compounds, the Si–S bonds trans to the (pseudo)halogeno ligands [2.3944(10)–2.4452(11) Å] are

dx.doi.org/10.1021/ic401698a | *Inorg. Chem.* 2013, 52, 10664–10676

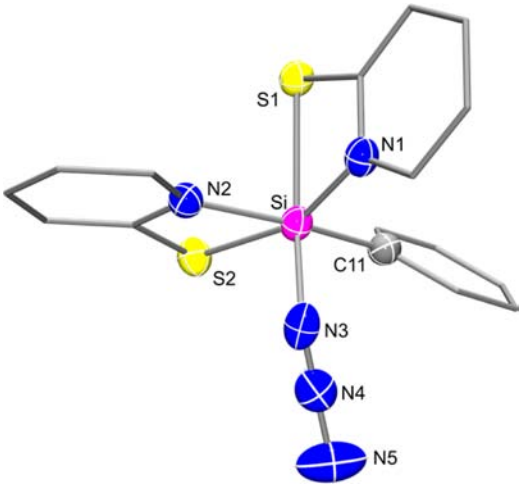

Figure 5. Molecular structure of **8** in the crystal (probability level of displacement ellipsoids 50%). Selected bond lengths (Å) and angles (deg): Si–S1 2.4248(9), Si–S2 2.3060(10), Si–N1 1.908(2), Si–N2 1.949(2), Si–N3 1.885(2), Si–C11 1.902(2), N3–N4 1.076(3), N4–N5 1.194(4); S1–Si–S2 93.42(3), S1–Si–N1 70.25(7), S1–Si–N2 86.61(7), S1–Si–N3 161.52(9), S1–Si–C11 92.67(8), S2–Si–N1 159.03(7), S2–Si–N2 71.97(7), S2–Si–N3 100.94(8), S2–Si–C11 95.96(9), N1–Si–N2 93.39(9), N1–Si–N3 92.92(10), N1–Si–C11 97.81(11), N2–Si–N3 86.85(9), N2–Si–C11 167.83(11), N3–Si–C11 97.28(10), Si–N3–N4 128.8(2), N3–N4–N5 175.2(3).

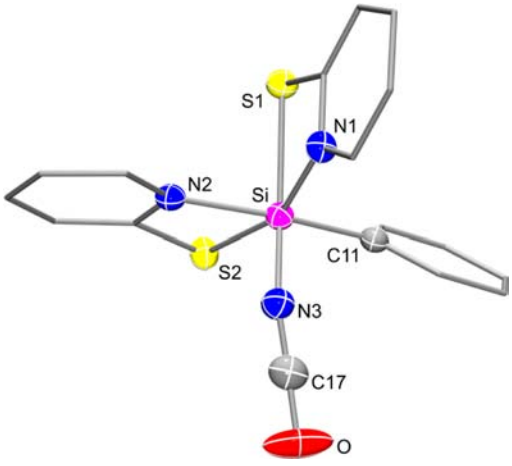

Figure 6. Molecular structure of **9** in the crystal (probability level of displacement ellipsoids 50%). Selected bond lengths (Å) and angles (deg): Si–S1 2.4436(11), Si–S2 2.3087(11), Si–N1 1.906(3), Si–N2 1.939(2), Si–N3 1.800(3), Si–C11 1.899(3), O–C17 1.191(4), N3–C17 1.171(4); S1–Si–S2 92.10(4), S1–Si–N1 70.12(7), S1–Si–N2 86.92(7), S1–Si–N3 162.67(10), S1–Si–C11 92.36(9), S2–Si–N1 157.55(8), S2–Si–N2 71.91(7), S2–Si–N3 101.84(9), S2–Si–C11 96.65(10), N1–Si–N2 92.91(10), N1–Si–N3 93.74(11), N1–Si–C11 97.65(11), N2–Si–N3 87.68(10), N2–Si–C11 168.49(12), N3–Si–C11 96.15(12), Si–N3–C17 155.8(3), N3–C17–O 178.1(4).

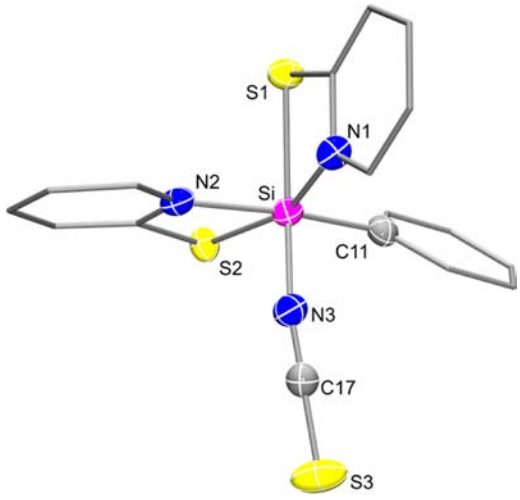

Figure 7. Molecular structure of **10** in the crystal (probability level of displacement ellipsoids 50%). Selected bond lengths (Å) and angles (deg): Si–S1 2.3944(10), Si–S2 2.3029(10), S3–C17 1.594(3), Si–N1 1.897(2), Si–N2 1.940(2), Si–N3 1.829(2), Si–C11 1.905(3), N3–C17 1.172(3); S1–Si–S2 94.51(4), S1–Si–N1 71.29(7), S1–Si–N2 88.50(6), S1–Si–N3 163.57(8), S1–Si–C11 94.26(8), S2–Si–N1 159.69(8), S2–Si–N2 72.06(7), S2–Si–N3 98.54(8), S2–Si–C11 97.82(8), N1–Si–N2 92.60(9), N1–Si–N3 93.46(10), N1–Si–C11 97.67(10), N2–Si–N3 86.07(9), N2–Si–C11 169.72(11), N3–Si–C11 93.82(11), Si–N3–C17 165.0(2), N3–C17–S3 179.6(3).

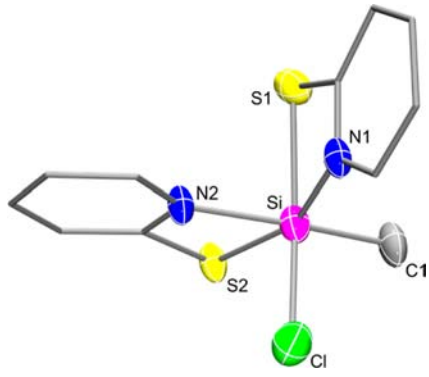

Figure 8. Molecular structure of **11** in the crystal (occupation factor 83%; probability level of displacement ellipsoids 50%). Selected bond lengths (Å) and angles (deg): Si–Cl 2.1980(19), Si–S1 2.4088(19), Si–S2 2.337(3), Si–N1 1.923(3), Si–N2 1.949(3), Si–C1 1.894(4); Cl–Si–S1 162.69(9), Cl–Si–S2 98.86(12), Cl–Si–N1 93.69(15), Cl–Si–N2 87.22(11), Cl–Si–C1 95.39(17), S1–Si–S2 93.39(12), S1–Si–N1 71.01(15), S1–Si–N2 85.12(11), S1–Si–C1 94.73(16), S2–Si–N1 157.9(2), S2–Si–N2 71.48(13), S2–Si–C1 98.93(17), N1–Si–N2 91.2(2), N1–Si–C1 97.9(2), N2–Si–C1 170.4(2). The structure of **11** is disordered (interchanged positions of Cl and S1) with a second molecule (occupation factor 17%) that represents the antipode of the enantiomer depicted above. The molecular structures of the two enantiomers are very similar.

0.0718–0.1350 Å longer than the Si–S bonds trans to the nitrogen ligand atom [2.3006(17)–2.337(3) Å]. Generally, the Si–S bond distances observed for **4**–**6** and **8**–**11** are very similar or slightly longer than those reported for axial Si–S bonds in five-coordinate[2a,c,d,i,m] and Si–S bonds in six-coordinate silicon(IV) complexes.[2g,h] The Si–N bond lengths of **4**–**6** and **8**–**11** are in the range of 1.890(4)–1.976(4) Å. The two Si–N distances of **4** [both 1.949(3) Å] and **5a** [1.954(3) and 1.973(3) Å] are identical or differ only slightly, whereas the two Si–N bond lengths of **5b**, **6**, and **8**–**11** differ by 0.026–0.055 Å. In all cases, the Si–N distances trans to the sulfur ligand atom [1.890(4)–1.923(3) Å] are shorter than those trans to the carbon ligand atom [1.939(2)–1.950(3) Å].

The structure of the cation of **12** is characterized by crystallographic C_2 symmetry. The silicon-coordination polyhedron is a strongly distorted trigonal bipyramid with the two nitrogen ligand atoms in the axial positions. The maximum

dx.doi.org/10.1021/ic401698a | *Inorg. Chem.* 2013, 52, 10664–10676

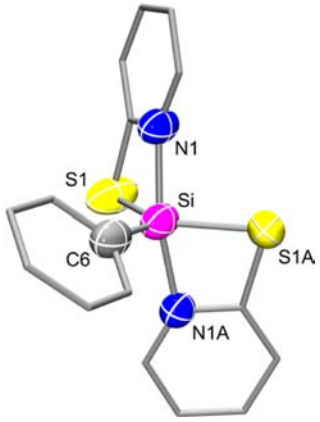

Figure 9. Molecular structure of the cation in the crystal of **12** (probability level of displacement ellipsoids 50%). Selected bond lengths (Å) and angles (deg): Si–S1 2.180(2), Si–S1A 2.180(2), Si–N1 1.944(4), Si–N1A 1.944(4), Si–C6 1.848(10); S1–Si–S1A 117.77(16), S1–Si–N1 74.69(14), S1–Si–N1A 94.81(15), S1–Si–C6 121.11(8), S1A–Si–N1 94.81(15), S1A–Si–N1A 74.69(14), S1A–Si–C6 121.11(8), N1–Si–N1A 159.9(3), N1–Si–C6 100.04(17), N1A–Si–C6 100.04(17).

Scheme 5. Four Possible Diastereomers (A–D) of Compounds 4–11

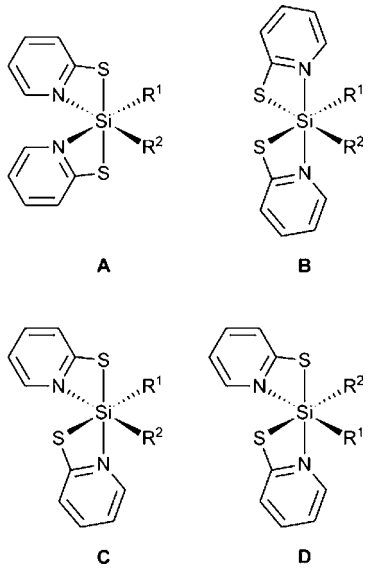

deviations from the ideal 90°, 120°, and 180° angles amount to 15.31(14)°, 2.23(16)°, and 20.1(3)°, respectively. The sum of the equatorial bond angles is 360.0°, and the Berry distortion[10] amounts to 21.9%. The two chelating *N*,*S*-pyridine-2-thiolato ligands and the silicon-coordination center build up two highly strained four-membered SiSCN chelate rings, with S–Si–N bite angles of 74.69(14)°. This value, however, is somewhat higher than those observed for the six-coordinate silicon(IV) complexes **4–6** and **8–11** [69.95(9)–72.55(9)°]. The two Si–S bond distances of **12** [both 2.180(2) Å] are significantly shorter than those observed for **4–6** and **8–11** [2.3006(17)–2.337(3) and 2.3944(10)–2.4451(11) Å] but very similar to those reported for equatorial Si–S bonds in five-coordinate silicon(IV) complexes.[2a,c–e,i,l,m] The two Si–N bond distances of **12** [both 1.994(4) Å] are somewhat longer than those observed for **4–6** and **8–11** [1.890(4)–1.976(4) Å].

NMR Spectroscopic Studies. Compounds **4–12** were studied by NMR spectroscopy in the solid state (^{15}N, ^{19}F, and ^{29}Si) and (except **4**) in solution (^{1}H, ^{13}C, ^{19}F, and ^{29}Si; solvent, CD_2Cl_2). The data obtained (see the Experimental Section) confirm the identities of these compounds.

As can be seen from Table 1, the isotropic ^{29}Si chemical shifts of **5–11** in the solid state and in solution are very similar,

Table 1. Isotropic ^{29}Si Chemical Shifts (ppm) of 4–12 in the Solid State (T = 22 °C) and in Solution (T = 23 °C; Solvent, CD_2Cl_2)

compound	δ^{29}Si (solid state)	δ^{29}Si (solution)
4	−182.2 to −177.4	*a*
5	−156.9 to −153.4, −152.9 to −149.0[b]	−154.1
6	−150.2[c]	−149.0[d]
7	−167.8 to −160.0[b]	−164.4
8	−156.2	−153.9
9	−165.5	−163.7
10	−170.3	−168.7
11	−150.1 to −149.4[b]	−148.3
12	−76.5	−77.2[e]

[a]Insoluble in common deuterated organic solvents. [b]Multiplet due to dipolar coupling. [c]Doublet, $^{1}J(^{29}Si,^{19}F)$ = 268 Hz. [d]Doublet, $^{1}J(^{29}Si,^{19}F)$ = 275 Hz. [e]Spectrum recorded at −70 °C.

indicating that the six-coordinate silicon(IV) complexes exist also in solution. This assumption is further supported by all of the other NMR spectroscopic data obtained (see the Experimental Section). The isotropic ^{29}Si chemical shifts of **12** in the solid state and in solution are also very similar (Table 1), indicating that the five-coordinate silicon(IV) complex **12** exists in solution as well. Compound **5** shows two ^{29}Si resonance signals in the solid state, which is in agreement with the results of the crystal structure analysis (cocrystallization of the two diastereomers **5a** and **5b**). NMR spectroscopic data for compound **4** in solution could not be obtained because of its poor solubility in common deuterated organic solvents. The ^{29}Si NMR spectrum of **12** in solution was recorded at −70 °C because of its strongly pronounced dynamic behavior at 23 °C (no signal detected at 23 °C). The range of the isotropic ^{29}Si chemical shifts of **4–11** indicates a strong influence of the different monodentate ligands on the ^{29}Si chemical shift. As can be seen from the similar isotropic ^{29}Si chemical shifts of the two diastereomers **5a** and **5b** in the solid state, the different relative arrangements of the two sulfur ligand atoms (**5a**, trans; **5b**, cis) only slightly affect the ^{29}Si chemical shift.

A comparison of the isotropic ^{15}N chemical shifts of compounds **4–12** in the solid state shows that the two pyridine-nitrogen atoms of **4–11** differ from each other (Table 2). For the more symmetrical dichloro complex **4**, the shift difference is relatively small (3.0 ppm), whereas the shift differences for **5–11** are much larger ($\Delta\delta^{29}$Si = 23.6–27.6 ppm). For the C_2-symmetrical silicon(IV) complex **12**, only one ^{15}N resonance signal for the two pyridine-nitrogen atoms was observed. Contrary to the solid-state ^{29}Si NMR spectrum of **5** (two resonance signals), the ^{15}N NMR spectrum of **5** does not show separate resonance signals for the two diastereomers (only two out of four expected resonance signals were observed).[11] The isotropic ^{15}N chemical shifts of the nitrogen atoms of the cyanato-*N*, thiocyanato-*N*, or azido ligands of **8–10** are within the expected ranges.

dx.doi.org/10.1021/ic401698a | *Inorg. Chem.* 2013, 52, 10664–10676

Table 2. Isotropic ^{15}N Chemical Shifts (ppm) of 4−12 in the Solid State (T = 22 °C)

compound	δ^{15}N (pyridine-2-thiolato ligands)	δ^{15}N (pseudohalogeno ligand)
4	−110.7, −107.7	
5	−133.8, −110.2	
6	−135.7, −109.6	
7	−133.5, −109.1	
8	−135.5, −107.9	−303.2 (*N*NN), −208.4 (NN*N*), −138.4 (N*N*N)
9	−134.8, −110.0	−325.7 (*N*CO)
10	−136.0, −110.7	−233.9 (*N*CS)
11	−129.8, −104.5	
12	−126.6	

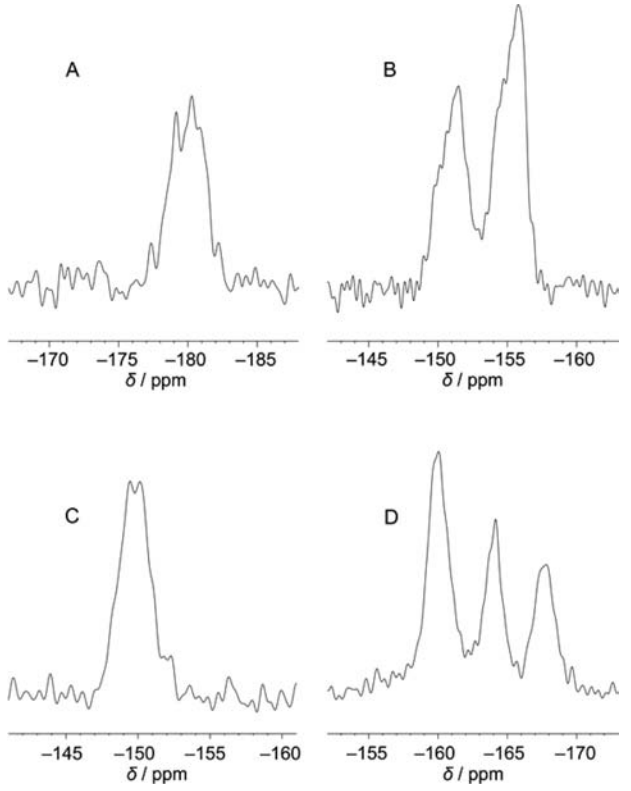

Figure 10. ^{29}Si VACP/MAS NMR spectra of (A) **4**, (B) **5**, and (C) **11** (ν_{rot} = 10 kHz; T = 22 °C) and (D) the ^{29}Si HPDec/MAS NMR spectrum of **7** (ν_{rot} = 6.8 kHz; T = 22 °C).

As shown in Figure 10, the resonance signals in the solid-state ^{29}Si NMR spectra of the chlorosilicon(IV) complexes **4**, **5**, and **11** and the bromosilicon(IV) complex **7** are broadened because of $^{1}J(^{29}\text{Si,X})$ couplings [X = ^{35}Cl (I = $^{3}/_{2}$), ^{37}Cl (I = $^{3}/_{2}$); ^{79}Br (I = $^{3}/_{2}$), ^{81}Br (I = $^{3}/_{2}$)]. In addition, it is well-known that magic angle spinning (MAS) fails to eliminate the effect of dipolar coupling for spin $^{1}/_{2}$ nuclei completely when coupled to quadrupole nuclei with a quadrupole frequency comparable to the Zeeman frequency of the nuclei.[12] The spectrum of **5** shows two resonance signals (intensity ratio 1:1) due to the presence of two diastereomers.

The ^{29}Si NMR spectrum of compound **5** in solution (solvent, CD_2Cl_2) shows one resonance signal at 23 °C (−154.1 ppm), whereas the solid-state NMR studies and the crystal structure analysis revealed the existence of two diastereomers in the crystal (molar ratio 1:1). To get more information about the stereochemistry of **5** in solution (solvent, CD_2Cl_2), variable-temperature NMR studies were performed. Upon cooling from 23 to −70 °C, the ^{29}Si resonance signal splits into two signals (−156.4 and −155.4 ppm; intensity ratio ca. 4:1; Figure 11),

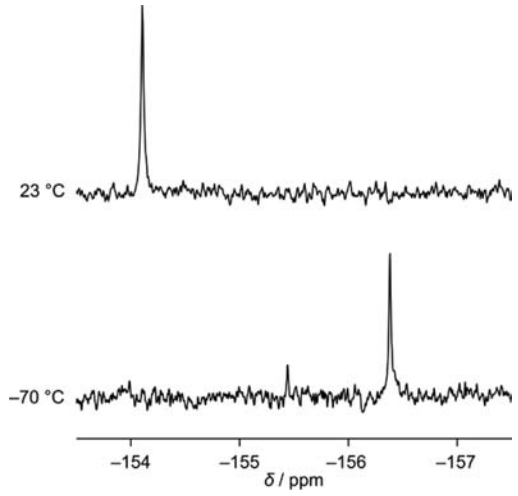

Figure 11. Temperature dependence of the ^{29}Si NMR spectrum of **5** (CD_2Cl_2; 99.4 MHz). The temperature dependence of the ^{29}Si NMR spectrum is completely reversible upon heating.

indicating the existence of two diastereomers that are configurationally stable on the NMR time scale at this temperature. Figure 12 shows the temperature dependence of the ^{1}H NMR spectrum of **5** in the temperature range of 23 to −70 °C (solvent, CD_2Cl_2), indicating a dynamic behavior, which can be interpreted in terms of an isomerization process (interconversion of the diastereomers **5a** and **5b**). At −70 °C, there are also two sets of resonance signals in the ^{1}H NMR spectrum (intensity ratio 4:1; Figures 12 and 13), again indicating the existence of two diastereomers. This result is in agreement with that obtained in the low-temperature ^{29}Si NMR studies of **5** (see above). On the basis of the results of quantum-chemical investigations (see the Computational Studies section), the dominating species can be assigned to isomer **C** (**5b**) and the other species to isomer **A** (**5a**).

As observed for **5**, the ^{1}H, ^{13}C, and ^{29}Si NMR spectra of **6**−**11** show only one set of resonance signals each at 23 °C (solvent, CD_2Cl_2), whereas two sets of ^{1}H resonance signals were observed at −70 °C (except for **11**; only one set of ^{1}H resonance signals) with intensity ratios of about 18:1 (**6**), 1.2:1 (**7**), 8:1 (**8**), 17:1 (**9**), or 3:1 (**10**) (intensity ratios extracted from the ^{1}H NMR spectra). The interpretation of these findings is analogous to that given for **5**. In the ^{1}H, ^{13}C, and ^{29}Si NMR spectra of the ionic compound **12**, only one set of resonance signals each was observed at −70 °C.

Computational Studies. To further support and rationalize the experimental findings obtained in the crystal structure analyses and NMR spectroscopic studies of **5**−**10** and **12**, we have conducted theoretical analyses of the structure, stability, and bonding of various silicon(IV) complexes Si(SC$_5$H$_4$N)$_2$PhX with X = F, Cl, Br, I, N$_3$, NCO, and NCS in the gas phase and in a dichloromethane solution using relativistic density functional theory (DFT).

All calculations were performed with the Amsterdam Density Functional (*ADF*) program,[13] using relativistic DFT at ZORA-BP86/TZ2P for geometry optimization and energies.[14,15] Solvation in dichloromethane was simulated using the

dx.doi.org/10.1021/ic401698a | *Inorg. Chem.* 2013, 52, 10664−10676

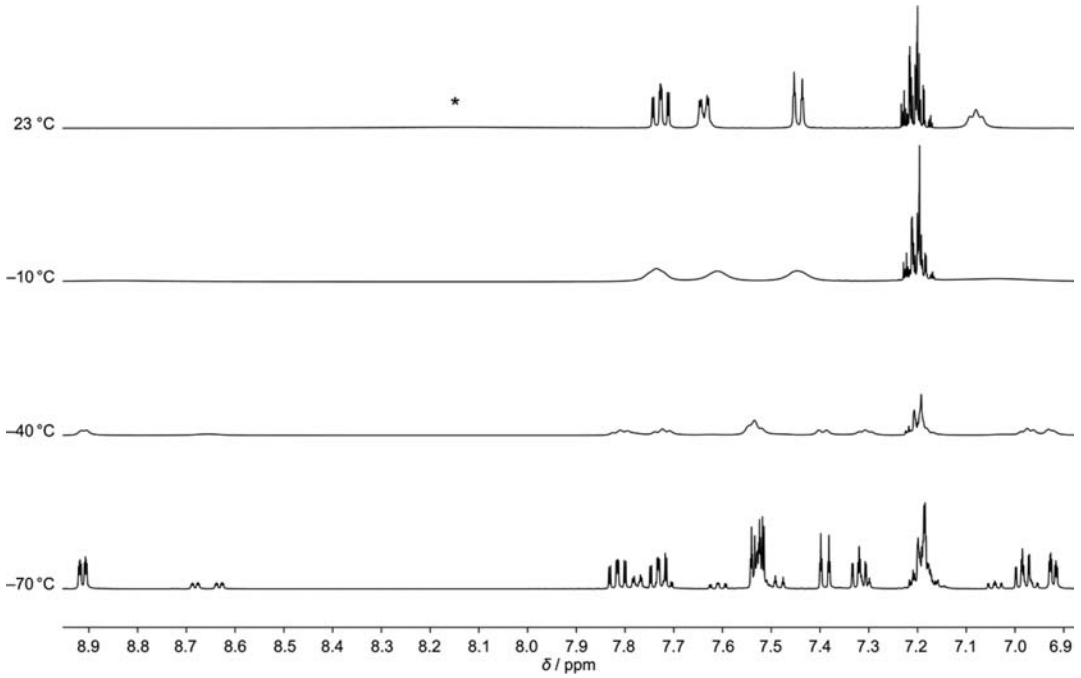

Figure 12. Temperature dependence of the ^{1}H NMR spectrum of **5** in the temperature range of 23 to −70 °C (CD_2Cl_2; 500.1 MHz). The temperature dependence of the ^{1}H NMR spectrum is completely reversible upon heating (the asterisk indicates the broad resonance signal of the pyridine *H*-6 protons at ca. 8.15 ppm).

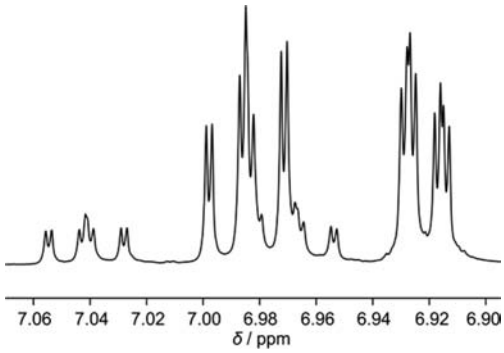

Figure 13. Partial ^{1}H NMR spectrum of **5** at −70 °C (CD_2Cl_2; 500.1 MHz), showing the resonance signals of two protons of each of the two diastereomers (molar ratio 4:1).

conductor-like screening model (COSMO).[16] All stationary points were verified to be minima on the potential energy surface through vibrational analysis. The bonding mechanism was analyzed within the framework of quantitative Kohn−Sham molecular orbital (MO) theory in combination with a quantitative energy decomposition analysis (EDA) of the interaction energy ΔE_{int} of selected bonds into classical electrostatic attraction ΔV_{elstat}, Pauli repulsion ΔE_{Pauli} between occupied orbitals, and stabilizing orbital interactions ΔE_{oi}, such as highest occupied molecular orbital (HOMO)−lowest unoccupied molecular orbital (LUMO) interaction (for details, see ref 17). Atomic charges were computed using the Voronoi Deformation Density (VDD) method developed by Bickelhaupt et al.[18]

The computed structures and relative energies of the four diastereomers **A**−**D** of the studied silicon(IV) complexes $Si(SC_5H_4N)_2PhX$ in CH_2Cl_2 are collected in Figures 14 and 15. The four diastereomers have, for each X, stabilities with a maximum span in relative energies of 6.4 kcal mol^{-1} in the case of X = N_3 (Figure 15). In all cases, isomers **A** and **C** are more stable than **B** and **D**. Here, we are mainly interested in the relative stability of **A** with respect to **C** as a function of ligand X.

The computations confirm the experimental observation that for compounds **5**−**10** two diastereomers are observed in solution (CD_2Cl_2) at −70 °C, one of which is dominating. According to the calculated relative energies, these species are the diastereomers **A** and **C**, with **C** being the dominating one (Figures 14 and 15). Furthermore, the results of the computational studies are also in agreement with the experimental observation that the diastereomers of **5** (**5a**, type **A**; **5b**, type **C**) cocrystallize; in fact, the calculated energy difference between **A** and **C** (0.8 kcal mol^{-1}) is very small and represents the smallest one in the series of compounds studied experimentally by single-crystal X-ray diffraction. In the case of **6** and **8**−**10** (energy difference between **A** and **C**, 1.6−2.8 kcal mol^{-1}), only diastereomer **C** was observed in the crystal.

The computational studies, furthermore, show that, for the silicon(IV) complexes with X = F, Cl, Br, and I, the viability of diastereomer **A** further increases upon going from X = F to I. In the case of the not yet synthesized complex with X = I [we rather isolated the five-coordinate ionic silicon(IV) complex **12**], diastereomer **A** is even slightly more favorable than **C**. Thus, the relative stabilities of **A** relative to **C** are 1.7 (F), 0.8 (Cl), 0.2 (Br), and −0.3 kcal mol^{-1} (I), respectively (Figure 14). Note that for all ligands X, except X = I, **C** is the most stable diastereomer. In the case of the three pseudohalogeno ligands coordinating via a nitrogen atom (X = N_3, NCO, NCS), diastereomer **A** is destabilized relative to **C** by 1.6−2.8 kcal mol^{-1} (Figure 15), that is, by an amount similar to that in the case of X = F or even more.

The Si−X bond distance in diastereomer **C** increases from ca. 1.68 to 2.71 Å along X = F, Cl, Br, and I (Figure 14), and the Si−N bond distance in the three compounds with ligands coordinating via a nitrogen atom (X = N_3, NCO, NCS)

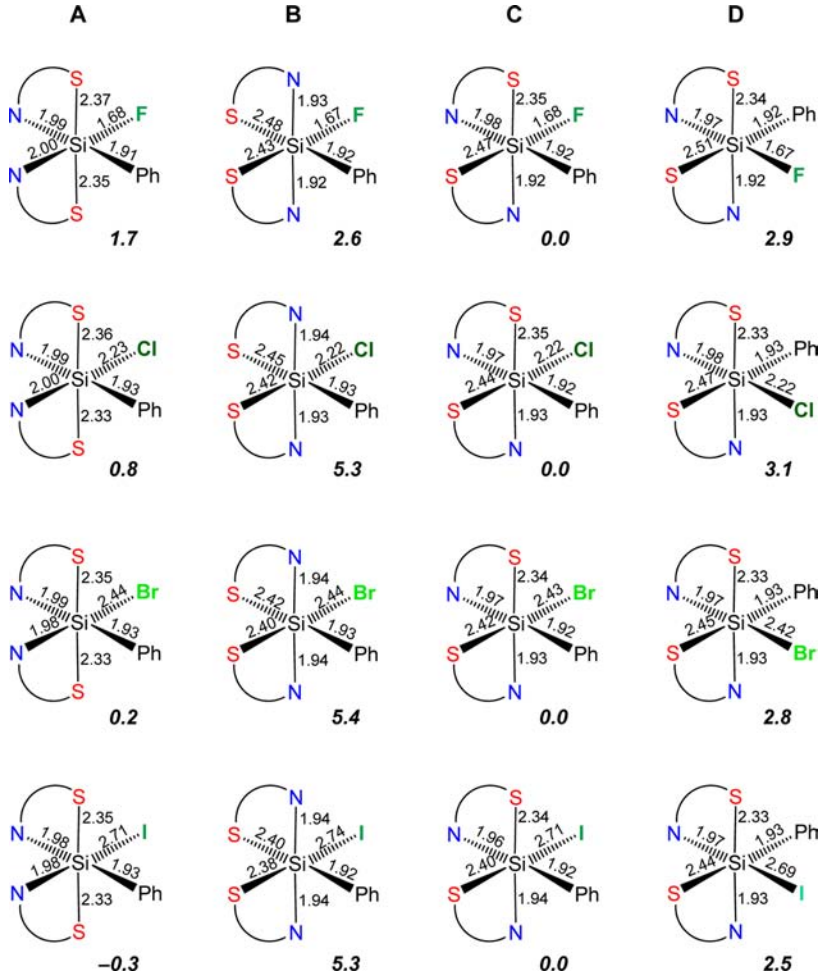

Figure 14. Relative energies (kcal mol^{-1}) and bond lengths (Å) of the isomers **A**–**D** of the silicon(IV) complexes $Si(SC_5H_4N)_2PhX$ (X = F, Cl, Br, I), computed at ZORA-BP86/TZ2P with COSMO for simulating solvation in CH_2Cl_2.

amounts to 1.80–1.85 Å (Figure 15). For a given ligand X, the variation in the Si–X bond distance along the isomers **A**–**D** is relatively small, between 0.01 Å for X = F and 0.05 Å for X = I with its weaker and softer Si–I bond. The silicon–element bonds to the *N*,*S*-pyridine-2-thiolato and phenyl ligands are relatively constant in all complexes (diastereomers **A**–**D**), with values of 1.91–1.93 Å for Si–C and 1.92–2.02 Å for Si–N and a somewhat larger range for Si–S (2.33–2.52 Å; Figures 14 and 15). Generally, the calculated silicon–element bond distances of diastereomers **A** and **C** are in reasonable agreement with the experimental data obtained in the crystal structure analyses of **5**, **6**, and **8**–**10** (Figures 2–7).

The above trend in the relative stability between diastereomers **A** and **C** is clear yet also subtle because it refers to differences in energy of about a few to only a few tenths of a kilocalorie per mole. We have, nevertheless, tried to shed light on its origin through analysis of the Si–X bond between $Si(SC_5H_4N)_2Ph^+$ and X^- in eight representative model systems, diastereomers **A** and **C** for the cases with X = F, Cl, Br, and I, in the gas phase using quantitative Kohn–Sham MO theory in combination with a bond EDA. Heterolytic dissociation of X^- from either **A** or **B** yields the cation **AB**, whereas from either **C** or **D**, this yields the cation **CD** (Scheme 6 and Figure 16). Both cationic species have a distorted square-pyramidal structure.

Interestingly, cation **AB** is 6.5 kcal mol^{-1} more stable than **CD**. This order in stability is inverted only after formation of the Si–X bond, which is substantially stronger for X^- interacting with **CD** than with **AB** (Table 3). For example, the Si–F bond strength between **CD** and F^- is −169.3 kcal mol^{-1}, while between **AB** and F^-, it amounts to only −161.6 kcal mol^{-1}. This leads to inversion from −6.5 kcal mol^{-1} in favor of **AB** relative to **CD** to +1.3 kcal mol^{-1} against **A** relative to **C** in the gas phase, as shown in Figure S1 in the Supporting Information (in CH_2Cl_2; this value is 1.7 kcal mol^{-1} against **A** relative to **C**; Figure 14). EDA in Table 3 shows that the Si–F bond in **C** is stronger than that in **A** because of somewhat less steric (Pauli) repulsion ΔE_{Pauli} and a more favorable electrostatic attraction term ΔV_{elstat}. This suggests that there is slightly less steric congestion in **C** than in **A**, a subtle effect that is not easily revealed by simple inspection of the structures in Figures 2, 3, and 14.

The fact that, along X = F, Cl, Br, and I, the energy of **A** decreases relative to that of **C** can be understood in terms of the decreasing Si–X bond strength. This has the consequence that, while the Si–X bond always remains stronger in **C**, the absolute difference in the Si–X bond strengths between **A** and **C** becomes smaller and, for X = I, can no longer invert the stability order between **AB** and **CD**, which is 6.5 kcal mol^{-1} in favor of the former. The heterolytic Si–X bond strength decreases along the anionic halogeno ligands because the electron-donating capability of their valence p atomic orbital decreases along X = F, Cl, Br, and I. This trend is reinforced by

dx.doi.org/10.1021/ic401698a | *Inorg. Chem.* 2013, 52, 10664–10676

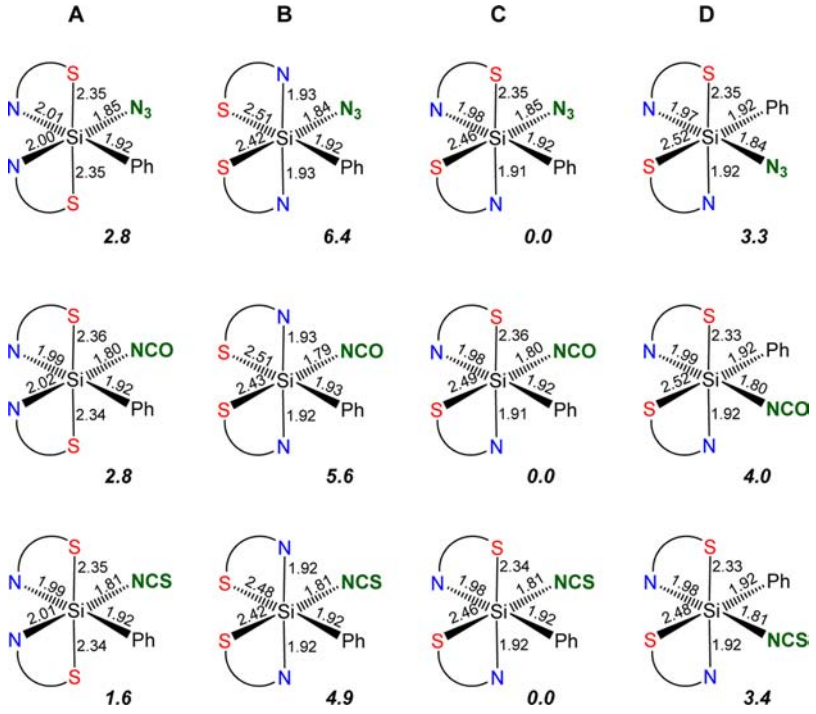

Figure 15. Relative energies (kcal mol^{-1}) and bond lengths (Å) of the isomers **A**–**D** of the silicon(IV) complexes $Si(SC_5H_4N)_2PhX$ (X = N_3, NCO, NCS), computed at ZORA-BP86/TZ2P with COSMO for simulating solvation in CH_2Cl_2.

Scheme 6. Isomers AB and CD of the Cation $Si(SC_5H_4N)_2Ph^+$

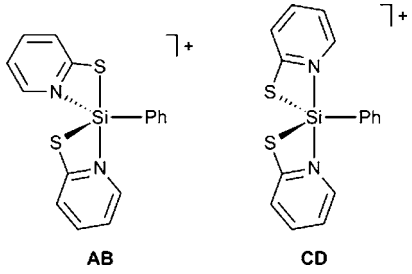

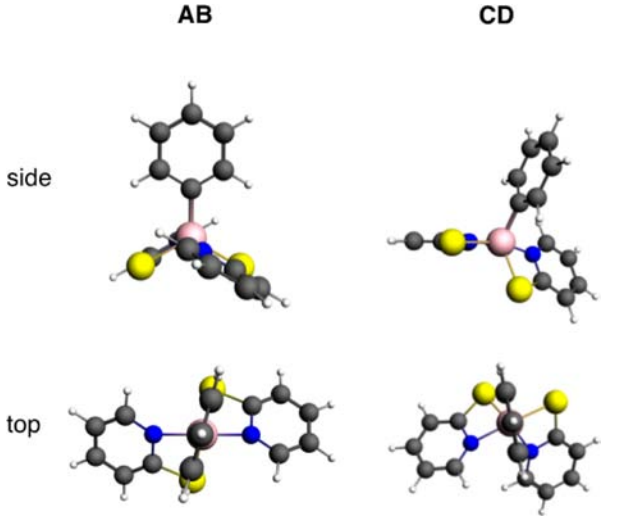

Figure 16. Side and top views of cations **AB** (resulting from removal of X^- from **A** or **B**) and **CD** (resulting from removal of X^- from **C** or **D**) computed at ZORA-BP86/TZ2P in the gas phase. Cation **AB** is 6.5 kcal mol^{-1} more stable than **CD**.

Table 3. Si–X Bond EDA (kcal mol^{-1}) and Silicon Atomic Charges (au) of Diastereomers A and C of the Silicon(IV) Complexes $Si(SC_5H_4N)_2PhX$ (X = F, Cl, Br, I) in the Gas Phase[a]

		F	Cl	Br	I
A	ΔE_{bond}	−161.6	−107.9	−96.2	−85.7
	ΔE_{prep}	37.1	37.4	36.4	35.1
	ΔE_{int}	−198.7	−145.3	−132.6	−120.8
	ΔE_{Pauli}	202.3	152.7	137.1	117.5
	ΔV_{elstat}	−257.6	−180.7	−163.7	−143.7
	ΔE_{oi}	−143.4	−117.3	−105.9	−94.5
	Q(Si) in cation **AB**′	+0.363	+0.364	+0.363	+0.362
C	ΔE_{bond}	−169.3	−115.2	−103.2	−92.3
	ΔE_{prep}	37.7	36.8	35.5	33.2
	ΔE_{int}	−207.0	−152.0	−138.7	−125.5
	ΔE_{Pauli}	199.0	151.1	135.2	117.1
	ΔV_{elstat}	−265.2	−188.9	−171.0	−150.9
	ΔE_{oi}	−140.8	−114.2	−102.9	−91.7
	Q(Si) in cation **CD**′	+0.351	+0.351	+0.350	+0.348

[a]Computed at ZORA-BP86/TZ2P (structures and energies) in the gas phase. EDA: $\Delta E_{bond} = \Delta E_{prep} + \Delta E_{int}$ and $\Delta E_{int} = \Delta E_{Pauli} + \Delta V_{elstat} + \Delta E_{oi}$. Q(Si) = VDD atomic charge of silicon in **AB**′ or **CD**′, that is, those cationic fragments in the geometry they adopt in the overall molecules **A** and **C**, respectively.

a weakening in the electrostatic attraction in the same order because of increasing Si–X bond distance as one goes from X = F to I. This has been discussed in more detail in earlier work, in which it was shown that for exactly the same reason the gas-phase proton affinity,[19] alkyl cation affinity,[20] and nucleophilicity decrease in the very same order.[21] The fact that the attempted synthesis of **12**′ instead yields **12** is consistent with the computational result that **12**′ contains by far the weakest silicon–halogen bond in the series studied.

dx.doi.org/10.1021/ic401698a | *Inorg. Chem.* 2013, 52, 10664–10676

Finally, we recall that our computations predict that the relative abundance of the $Si(SC_5H_4N)_2PhX$ diastereomer **A** relative to **C** further increases if one proceeds from X = F to Cl and Br and to the not yet synthesized species with X = I. For X = I, diastereomer **A** is even more stable than **C**. As an approximate indicator of these species' kinetic stabilities toward decomposition through bimolecular processes, we have computed the HOMO−LUMO gap in all silicon(IV) complexes $Si(SC_5H_4N)_2PhX$ (X = F, Cl, Br, I, N_3, NCO, NCS) both in the gas phase and in CH_2Cl_2 (Table 4). It

Table 4. HOMO−LUMO Gap (eV) of Diastereomers A−D of the Silicon(IV) Complexes $Si(SC_5H_4N)_2PhX$ (X = F, Cl, Br, I, N_3, NCO, NCS) in the Gas Phase and in CH_2Cl_2[a]

	X	A	B	C	D
gas phase	F	2.78	2.41	2.62	2.59
	Cl	2.77	2.36	2.62	2.57
	Br	2.69	2.35	2.62	2.49
	I	2.32	2.24	2.55	2.23
	N_3	2.69	2.41	2.62	2.63
	NCO	2.78	2.40	2.60	2.61
	NCS	2.51	2.36	2.60	2.50
CH_2Cl_2	F	2.95	2.61	2.85	2.81
	Cl	2.95	2.58	2.85	2.79
	Br	2.93	2.58	2.86	2.74
	I	2.81	2.52	2.83	2.60
	N_3	2.93	2.57	2.84	2.82
	NCO	2.95	2.56	2.81	2.80
	NCS	2.93	2.58	2.82	2.78

[a]Computed at ZORA-BP86/TZ2P (structures and energies) in the gas phase and solvated in CH_2Cl_2 (COSMO).

appears that the HOMO−LUMO gap of isomer **C** is essentially equal for all X, i.e., ca. 2.8−2.9 eV in CH_2Cl_2. Also for diastereomer **A**, the HOMO−LUMO gap decreases only slightly from 3.0 eV (X = F, Cl) via 2.9 eV (X = Br) to 2.8 eV (X = I).

CONCLUSION

With the synthesis of compounds **4**−**11**, a series of novel neutral six-coordinate silicon(IV) complexes with $SiS_2N_2Cl_2$, SiS_2N_2FC, SiS_2N_2ClC, SiS_2N_2BrC, and SiS_2N_3C skeletons has been made available. Compound **12** represents a novel cationic five-coordinate silicon(IV) complex with a SiS_2N_2C skeleton. To the best of our knowledge, compounds **4**−**12** are the first silicon(IV) complexes with bidentate monoanionic *N*,*S*-pyridine-2-thiolato(−) ligands. Compounds **5**−**12** exist both in the solid state and in solution, whereas **4** could only be studied in the solid state because of its poor solubility. In the case of **5**, two diastereomers (**5a** and **5b**) cocrystallize (molar ratio 1:1). The silicon-coordination polyhedra of **4**−**6** and **8**−**11** in the crystal are best described as strongly distorted octahedra, with the two sulfur atoms in trans (**4** and diastereomer **5a**) or cis position (diastereomer **5b**, **6**, and **8**−**11**). The silicon-coordination polyhedron of **12** is a strongly distorted trigonal bipyramid with the two nitrogen ligand atoms in the axial sites. The experimental results are supported and explained by our quantum-chemical computations and bonding analyses based on relativistic DFT. Experimental and computed structures agree well. The computations reveal that trends in product distributions (diastereomers of **5**−**10** and the formation of **12** instead of the targeted **12′**) can be understood on the basis of the heterolytic silicon−(pseudo)halogeno bond strength.

EXPERIMENTAL SECTION

General Procedures. All syntheses were carried out under a dry argon atmosphere in oven-dried glassware using standard Schlenk techniques. The organic solvents used were dried and purified according to standard procedures. Solution ^1H, $^{13}C\{^1H\}$, $^{19}F\{^1H\}$, and $^{29}Si\{^1H\}$ NMR spectra were recorded at 23 °C (if not specified otherwise) on a Bruker Avance 500 (^1H, 500.1 MHz; ^{13}C, 125.8 MHz; ^{29}Si, 99.4 MHz), Bruker Avance 400 (^{19}F, 376.5 MHz), or Bruker DRX-300 (^1H, 300.1 MHz; ^{13}C, 75.5 MHz; ^{29}Si, 59.6 MHz) NMR spectrometer. CD_2Cl_2 was used as the solvent. Chemical shifts (ppm) were determined relative to internal $CDHCl_2$ (^1H, δ 5.32), internal CD_2Cl_2 (^{13}C, δ 53.8), external $CFCl_3$ (^{19}F, δ 0), or external tetramethylsilane (^{29}Si, δ 0). Assignment of the ^1H and ^{13}C NMR data was supported by $^1H-^1H$ and $^1H-^{13}C$ correlation and DEPT 135 experiments. The thermocouple used with the probe for the variable-temperature NMR studies was calibrated for lower temperatures according to ref 22 using a 4% solution of MeOH in $[D_4]$MeOH containing a trace of HCl. Solid-state ^{15}N and ^{29}Si VACP/MAS, ^{29}Si HPDec/MAS, and ^{19}F MAS NMR spectra were recorded at 22 °C on a Bruker DSX-400 NMR spectrometer with bottom layer rotors of ZrO_2 (diameter, 4 or 7 mm) containing ca. 50 mg (4 mm) or ca. 250 mg (7 mm) of sample [^{15}N, 40.6 MHz; ^{19}F, 376.5 MHz; ^{29}Si, 79.5 MHz; external standard, tetramethylsilane (^{29}Si, δ 0), glycine (^{15}N, δ −342.0), or CaF_2 (^{19}F, δ −108.0); spinning rate, 10 kHz (VACP/MAS), 6.8 kHz (HPDec/MAS), or 15 kHz (MAS); contact time, 5 ms (^{15}N, ^{29}Si); 90° ^1H transmitter pulse length, 2.6 μs (4 mm) or 3.6 μs (7 mm); repetition time, 5−15 s, depending on the relaxation times of the protons].

Dichlorobis[*N*,*S*-pyridine-2-thiolato(−)]silicon(IV) (4). Triethylamine (1.79 g, 17.7 mmol) and tetrachlorosilane (1.50 g, 8.83 mmol) were added at 20 °C in single portions one after another to a stirred solution of 2-pyridinethiol (1.96 g, 17.6 mmol) in tetrahydrofuran (40 mL), and the reaction mixture was then stirred at this temperature for 16 h. The resulting precipitate was filtered off, washed with tetrahydrofuran (2 × 10 mL), and discarded. The solvent of the filtrate (including the wash solutions) was removed in vacuo, followed by the addition of acetonitrile (25 mL). The resulting suspension was heated until a clear solution was obtained, which was then cooled slowly to 20 °C and kept undisturbed at this temperature for 2 days. The resulting colorless crystalline solid was isolated by filtration, washed with *n*-pentane (2 × 5 mL), and dried in vacuo (20 °C, 4 h, 0.01 mbar). Yield: 2.53 g (7.92 mmol, 90%). ^{15}N VACP/MAS NMR: δ −110.7, −107.7. ^{29}Si VACP/MAS NMR: δ −182.2 to −177.4. Anal. Calcd for $C_{10}H_8Cl_2N_2S_2Si$ (319.31): C, 37.62; H, 2.53; N, 8.77; S, 20.08. Found: C, 37.5; H, 2.6; N, 8.7; S, 19.6.

Chlorophenylbis[*N*,*S*-pyridine-2-thiolato(−)]silicon(IV) (5). Triethylamine (1.44 g, 14.2 mmol) and trichlorophenylsilane (1.50 g, 7.09 mmol) were added at 20 °C in single portions one after another to a stirred solution of 2-pyridinethiol (1.58 g, 14.2 mmol) in tetrahydrofuran (30 mL), and the reaction mixture was then stirred at this temperature for 16 h. The resulting precipitate was filtered off, washed with tetrahydrofuran (2 × 10 mL), and discarded. The solvent of the filtrate (including the wash solutions) was removed in vacuo, followed by the addition of acetonitrile (12 mL). The resulting suspension was heated until a clear solution was obtained, which was then cooled slowly to 20 °C and kept undisturbed at this temperature for 2 days. The resulting colorless crystalline solid was isolated by filtration, washed sequentially with diethyl ether (2 × 10 mL) and *n*-pentane (2 × 5 mL), and dried in vacuo (20 °C, 4 h, 0.01 mbar). Yield: 2.50 g (6.93 mmol, 98%). ^1H NMR (500.1 MHz): δ 7.07−7.09 (m, 2 H; *H*-5, SC_5H_4N), 7.17−7.24 (m, 3 H; *H*-3/*H*-4/*H*-5, C_6H_5), 7.44−7.46 (m, 2 H; *H*-3, SC_5H_4N), 7.63−7.65 (m, 2 H; *H*-2/*H*-6, C_6H_5), 7.70−7.74 (m, 2 H; *H*-4, SC_5H_4N), 8.14 (br s, 2 H; *H*-6, SC_5H_4N). $^{13}C\{^1H\}$ NMR (75.5 MHz): δ 118.1 (*C*-5, SC_5H_4N), 125.5 (*C*-3, SC_5H_4N), 127.3 (*C*-3/*C*-5, C_6H_5), 127.8 (*C*-4, C_6H_5), 132.6 (*C*-2/*C*-6, C_6H_5), 140.8 (*C*-6, SC_5H_4N), 141.3 (*C*-4, SC_5H_4N), 152.7 (*C*-

dx.doi.org/10.1021/ic401698a | Inorg. Chem. 2013, 52, 10664−10676

1, C_6H_5), 167.5 (*C*-2, SC_5H_4N). $^{29}Si\{^1H\}$ NMR (99.4 MHz): δ −154.1. ^{15}N VACP/MAS NMR: δ −133.8, −110.2. ^{29}Si VACP/MAS NMR: δ −156.9 to −153.4, −152.9 to −149.0. Anal. Calcd for $C_{16}H_{13}ClN_2S_2Si$ (360.96): C, 53.24; H, 3.63; N, 7.76; S, 17.77. Found: C, 53.1; H, 3.6; N, 7.8; S, 17.6.

Fluorophenylbis[*N*,*S*-pyridine-2-thiolato(−)]silicon(IV) (6). Fluorotrimethylstannane (977 mg, 5.34 mmol) was added at 20 °C in a single portion to a stirred solution of **5** (1.93 g, 5.35 mmol) in tetrahydrofuran (40 mL), and the reaction mixture was then stirred at this temperature for 2 h. The resulting precipitate was filtered off, washed with tetrahydrofuran (2 × 10 mL), and discarded, and the solvent of the filtrate (including the wash solutions) was removed in vacuo, followed by the addition of acetonitrile (35 mL). The resulting suspension was heated until a clear solution was obtained, which was then cooled slowly to 20 °C and kept undisturbed at this temperature for 2 days. The resulting colorless crystalline solid was isolated by filtration, washed sequentially with diethyl ether (2 × 10 mL) and *n*-pentane (2 × 5 mL), and dried in vacuo (20 °C, 4 h, 0.01 mbar). Yield: 1.54 g (4.47 mmol, 84%). ^1H NMR (500.1 MHz): δ 7.01−7.10 (m, 2 H; *H*-5, SC_5H_4N), 7.18−7.26 (m, 3 H; *H*-3/*H*-4/*H*-5, C_6H_5), 7.38−7.46 (m, 2 H; *H*-3, SC_5H_4N), 7.66−7.73 (m, 4 H; *H*-2/*H*-6, C_6H_5, and *H*-4, SC_5H_4N), 7.79 (br s, 2 H; *H*-6, SC_5H_4N). $^{13}C\{^1H\}$ NMR (125.8 MHz): δ 117.7 (*C*-5, SC_5H_4N), 125.7 (*C*-3, SC_5H_4N), 127.3 (*C*-3/*C*-5, C_6H_5), 128.0 (*C*-4, C_6H_5), 133.4 (*C*-2/*C*-6, C_6H_5), 140.9 (*C*-6, SC_5H_4N), 141.3 (*C*-4, SC_5H_4N), 150.1 (*C*-1, C_6H_5), 168.9 (*C*-2, SC_5H_4N). $^{19}F\{^1H\}$ NMR (376.5 MHz): δ −131.4 (br s; fwhh = 970 Hz). $^{29}Si\{^1H\}$ NMR (99.4 MHz): δ −149.0 (d, $^1J(^{29}Si,^{19}F)$ = 275 Hz). ^{15}N VACP/MAS NMR: δ −135.7, −109.6. ^{19}F MAS NMR: δ −139.4. ^{29}Si VACP/MAS NMR: δ −150.2 (d, $^1J(^{29}Si,^{19}F)$ = 268 Hz). Anal. Calcd for $C_{16}H_{13}FN_2S_2Si$ (344.51): C, 55.78; H, 3.80; N, 8.13; S, 18.62. Found: C, 55.3; H, 3.9; N, 8.1; S, 18.6.

Bromophenylbis[*N*,*S*-pyridine-2-thiolato(−)]silicon(IV) (7). Bromotrimethylsilane (1.06 g, 6.92 mmol) was added at 20 °C in a single portion to a stirred solution of **5** (1.00 g, 2.77 mmol) in acetonitrile (30 mL), and the reaction mixture was then stirred at 65 °C for 3 h and at 20 °C for 3 days. The solvent and the generated chlorotrimethylsilane were removed in vacuo, followed by the addition of acetonitrile (20 mL). The resulting suspension was heated until a clear solution was obtained, which was then cooled slowly to 20 °C and kept undisturbed at this temperature for 2 days. The resulting colorless crystalline solid was isolated by filtration, washed sequentially with diethyl ether (2 × 10 mL) and *n*-pentane (2 × 5 mL), and dried in vacuo (20 °C, 4 h, 0.01 mbar). Yield: 770 mg (1.89 mmol, 68%). ^1H NMR (500.1 MHz): δ 7.07−7.10 (m, 2 H; *H*-5, SC_5H_4N), 7.16−7.23 (m, 3 H; *H*-3/*H*-4/*H*-5, C_6H_5), 7.44−7.46 (m, 2 H; *H*-3, SC_5H_4N), 7.63−7.64 (m, 2 H; *H*-2/*H*-6, C_6H_5), 7.73−7.75 (m, 2 H; *H*-4, SC_5H_4N), 8.31 (br s, 2 H; *H*-6, SC_5H_4N). $^{13}C\{^1H\}$ NMR (125.8 MHz): δ 118.4 (*C*-5, SC_5H_4N), 125.2 (*C*-3, SC_5H_4N), 127.3 (*C*-3/*C*-5, C_6H_5), 127.9 (*C*-4, C_6H_5), 132.3 (*C*-2/*C*-6, C_6H_5), 140.9 (*C*-6, SC_5H_4N), 141.6 (*C*-4, SC_5H_4N), 153.1 (*C*-1, C_6H_5), 167.1 (*C*-2, SC_5H_4N). $^{29}Si\{^1H\}$ NMR (99.4 MHz): δ −164.4. ^{15}N VACP/MAS NMR: δ −133.5, −109.1. ^{29}Si HPDec/MAS NMR: δ −167.8 to −160.0. Anal. Calcd for $C_{16}H_{13}BrN_2S_2Si$ (405.41): C, 47.40; H, 3.23; N, 6.91; S, 15.82. Found: C, 47.7; H, 3.2; N, 7.1; S, 16.1.

Azidophenylbis[*N*,*S*-pyridine-2-thiolato(−)]silicon(IV) (8). Azidotrimethylsilane (361 mg, 3.13 mmol) was added at 20 °C in a single portion to a stirred solution of **5** (1.13 g, 3.13 mmol) in acetonitrile (30 mL), and the reaction mixture was then stirred at this temperature for 2 days. The solvent and the generated chlorotrimethylsilane were removed in vacuo, followed by the addition of acetonitrile (20 mL). The resulting suspension was heated until a clear solution was obtained, which was then cooled slowly to 20 °C and kept undisturbed at this temperature for 2 days. The resulting colorless crystalline solid was isolated by filtration, washed sequentially with diethyl ether (2 × 10 mL) and *n*-pentane (2 × 5 mL), and dried in vacuo (20 °C, 4 h, 0.01 mbar). Yield: 875 mg (2.38 mmol, 76%). ^1H NMR (300.1 MHz): δ 7.04−7.09 (m, 2 H; *H*-5, SC_5H_4N), 7.20−7.27 (m, 3 H; *H*-3/*H*-4/*H*-5, C_6H_5), 7.43−7.46 (m, 2 H; *H*-3, SC_5H_4N), 7.60−7.65 (m, 2 H; *H*-2/*H*-6, C_6H_5), 7.69−7.76 (m, 2 H; *H*-4, SC_5H_4N), 7.93 (br s, 2 H; *H*-6, SC_5H_4N). $^{13}C\{^1H\}$ NMR (75.5 MHz): δ 117.9 (*C*-5, SC_5H_4N), 125.7 (*C*-3, SC_5H_4N), 127.5 (*C*-3/*C*-5, C_6H_5), 128.0 (*C*-4, C_6H_5), 133.2 (*C*-2/*C*-6, C_6H_5), 140.9 (*C*-6, SC_5H_4N), 141.1 (*C*-4, SC_5H_4N), 149.2 (*C*-1, C_6H_5), 168.1 (*C*-2, SC_5H_4N). $^{29}Si\{^1H\}$ NMR (59.6 MHz): δ −153.9. ^{15}N VACP/MAS NMR: δ −303.2 (*N*NN), −208.4 (NN*N*), −138.4 (N*N*N), −135.5 (SC_5H_4N), −107.9 (SC_5H_4N). ^{29}Si VACP/MAS NMR: δ −156.2. Anal. Calcd for $C_{16}H_{13}N_5S_2Si$ (367.53): C, 52.29; H, 3.57; N, 19.06; S, 17.45. Found: C, 52.3; H, 3.5; N, 18.7; S, 17.3.

(Cyanato-*N*)phenylbis[*N*,*S*-pyridine-2-thiolato(−)]silicon(IV) (9). Potassium cyanate (195 mg, 2.40 mmol) was added at 20 °C in a single portion to a stirred solution of **5** (790 mg, 2.19 mmol) in acetonitrile (30 mL), and the reaction mixture was then stirred at this temperature for 3 days. The solvent was removed in vacuo, and dichloromethane (40 mL) was added to the residue. The resulting precipitate was filtered off, washed with dichloromethane (2 × 10 mL), and discarded, and the solvent of the filtrate (including the wash solutions) was removed in vacuo, followed by the addition of acetonitrile (15 mL). The resulting suspension was heated until a clear solution was obtained, which was then cooled slowly to 20 °C and kept undisturbed at this temperature for 2 days. The resulting colorless crystalline solid was isolated by filtration, washed sequentially with diethyl ether (2 × 10 mL) and *n*-pentane (2 × 5 mL), and dried in vacuo (20 °C, 4 h, 0.01 mbar). Yield: 710 mg (1.93 mmol, 88%). ^1H NMR (500.1 MHz): δ 7.05−7.07 (m, 2 H; *H*-5, SC_5H_4N), 7.19−7.27 (m, 3 H; *H*-3/*H*-4/*H*-5, C_6H_5), 7.42−7.44 (m, 2 H; *H*-3, SC_5H_4N), 7.64−7.67 (m, 2 H; *H*-2/*H*-6, C_6H_5), 7.69−7.72 (m, 2 H; *H*-4, SC_5H_4N), 7.89 (br s, 2 H; *H*-6, SC_5H_4N). $^{13}C\{^1H\}$ NMR (125.8 MHz): δ 117.9 (*C*-5, SC_5H_4N), 125.9 (*C*-3, SC_5H_4N), 127.4 (*C*-3/*C*-5, C_6H_5), 127.9 (*C*-4, C_6H_5), 132.9 (*C*-2/*C*-6, C_6H_5), 140.4 (*C*-6, SC_5H_4N), 141.0 (*C*-4, SC_5H_4N), 151.3 (*C*-1, C_6H_5), 168.4 (*C*-2, SC_5H_4N). $^{29}Si\{^1H\}$ NMR (99.4 MHz): δ −163.7. ^{15}N VACP/MAS NMR: δ −325.7 (*N*CO), −134.8 (SC_5H_4N), −110.0 (SC_5H_4N). ^{29}Si VACP/MAS NMR: δ −165.5. Anal. Calcd for $C_{17}H_{13}N_3OS_2Si$ (367.53): C, 55.56; H, 3.57; N, 11.43; S, 17.45. Found: C, 55.5; H, 3.5; N, 11.5; S, 17.4.

Phenyl(thiocyanato-*N*)bis[*N*,*S*-pyridine-2-thiolato(−)]silicon-(IV) (10). Potassium thiocyanate (482 mg, 4.96 mmol) was added at 20 °C in a single portion to a stirred solution of **5** (1.63 g, 4.52 mmol) in acetonitrile (40 mL), and the reaction mixture was then stirred at this temperature for 3 days. The solvent was removed in vacuo, and dichloromethane (40 mL) was added to the residue. The resulting precipitate was filtered off, washed with dichloromethane (2 × 10 mL), and discarded, and the solvent of the filtrate (including the wash solutions) was removed in vacuo, followed by the addition of acetonitrile (45 mL). The resulting suspension was heated until a clear solution was obtained, which was then cooled slowly to 20 °C and kept undisturbed at this temperature for 2 days. The resulting colorless crystalline solid was isolated by filtration, washed sequentially with diethyl ether (2 × 10 mL) and *n*-pentane (2 × 5 mL), and dried in vacuo (20 °C, 4 h, 0.01 mbar). Yield: 1.43 g (3.73 mmol, 83%). ^1H NMR (300.1 MHz): δ 7.08−7.13 (m, 2 H; *H*-5, SC_5H_4N), 7.22−7.29 (m, 3 H; *H*-3/*H*-4/*H*-5, C_6H_5), 7.44−7.48 (m, 2 H; *H*-3, SC_5H_4N), 7.60−7.66 (m, 2 H; *H*-2/*H*-6, C_6H_5), 7.72−7.78 (m, 2 H; *H*-4, SC_5H_4N), 8.02 (br s, 2 H; *H*-6, SC_5H_4N). $^{13}C\{^1H\}$ NMR (75.5 MHz): δ 118.4 (*C*-5, SC_5H_4N), 125.6 (*C*-3, SC_5H_4N), 127.6 (*C*-3/*C*-5, C_6H_5), 128.2 (*C*-4, C_6H_5), 133.0 (*C*-2/*C*-6, C_6H_5), 140.5 (*C*-6, SC_5H_4N), 141.5 (*C*-4, SC_5H_4N), 150.3 (*C*-1, C_6H_5), 167.6 (*C*-2, SC_5H_4N). $^{29}Si\{^1H\}$ NMR (99.4 MHz): δ −168.7. ^{15}N VACP/MAS NMR: δ −233.9 (*N*CS), −136.0 (SC_5H_4N), −110.7 (SC_5H_4N). ^{29}Si VACP/MAS NMR: δ −170.3. Anal. Calcd for $C_{17}H_{13}N_3S_3Si$ (383.59): C, 53.23; H, 3.42; N, 10.95; S, 25.08. Found: C, 53.2; H, 3.4; N, 10.9; S, 24.9.

Chloromethylbis[*N*,*S*-pyridine-2-thiolato(−)]silicon(IV) (11). Triethylamine (2.03 g, 20.1 mmol) and trichloromethylsilane (1.50 g, 10.0 mmol) were added at 20 °C in single portions one after another to a stirred solution of 2-pyridinethiol (2.23 g, 20.1 mmol) in tetrahydrofuran (40 mL), and the reaction mixture was then stirred at this temperature for 24 h. The resulting precipitate was filtered off, washed with tetrahydrofuran (2 × 10 mL), and discarded. The solvent of the filtrate (including the wash solutions) was removed in vacuo,

dx.doi.org/10.1021/ic401698a | *Inorg. Chem.* 2013, 52, 10664−10676

followed by the addition of acetonitrile (21 mL). The resulting suspension was heated until a clear solution was obtained, which was then cooled slowly to 20 °C and kept undisturbed at this temperature for 2 days. The resulting colorless crystalline solid was isolated by filtration, washed sequentially with diethyl ether (2 × 10 mL) and *n*-pentane (2 × 5 mL), and dried in vacuo (20 °C, 4 h, 0.01 mbar). Yield: 2.93 g (9.80 mmol, 98%). ^{1}H NMR (300.1 MHz): δ 1.12 (s, 3 H; CH_3), 6.99−7.04 (m, 2 H; *H*-5, SC_5H_4N), 7.39−7.43 (m, 2 H; *H*-3, SC_5H_4N), 7.67−7.73 (m, 2 H; *H*-4, SC_5H_4N), 7.99−8.01 (m, 2 H; *H*-6, SC_5H_4N). ^{13}C{^{1}H} NMR (75.5 MHz): δ 26.0 (*C*H_3), 117.9 (*C*-5, SC_5H_4N), 125.4 (*C*-3, SC_5H_4N), 140.4 (*C*-6, SC_5H_4N), 141.0 (*C*-4, SC_5H_4N), 168.1 (*C*-2, SC_5H_4N). ^{29}Si{^{1}H} NMR (59.6 MHz): δ −148.3. ^{15}N VACP/MAS NMR: δ −129.8, −104.5. ^{29}Si VACP/MAS NMR: δ −150.1 to −149.4. Anal. Calcd for $C_{11}H_{11}ClN_2S_2Si$ (298.89): C, 44.20; H, 3.71; N, 9.37; S, 21.46. Found: C, 44.1; H, 3.7; N, 9.3; S, 21.7.

Phenylbis[*N*,*S*-pyridine-2-thiolato(−)]silicon(IV) Iodide (12). Iodotrimethylsilane (1.39 g, 6.95 mmol) was added at 20 °C in a single portion to a stirred solution of **5** (1.00 g, 2.77 mmol) in acetonitrile (30 mL), and the reaction mixture was then stirred at 65 °C for 3 h and at 20 °C for 3 days. The solvent and the generated chlorotrimethylsilane were removed in vacuo, followed by the addition of acetonitrile (23 mL). The resulting suspension was heated until a clear solution was obtained, which was then cooled slowly to 20 °C and kept undisturbed at this temperature for 2 days. The resulting colorless crystalline solid was isolated by filtration, washed with *n*-pentane (2 × 5 mL), and dried in vacuo (20 °C, 4 h, 0.01 mbar). Yield: 832 mg (1.84 mmol, 66%). ^{1}H NMR (300.1 MHz): δ 7.33−7.39 (m, 2 H; *H*-3/*H*-5, C_6H_5), 7.41−7.42 (m, 1 H; *H*-4, C_6H_5), 7.43−7.48 (m, 2 H; *H*-5, SC_5H_4N), 7.61−7.66 (m, 2 H; *H*-2/*H*-6, C_6H_5), 7.72−7.75 (m, 2 H; *H*-3, SC_5H_4N), 8.10−8.15 (m, 2 H; *H*-4, SC_5H_4N), 8.26−8.29 (m, 2 H; *H*-6, SC_5H_4N). ^{13}C{^{1}H} NMR (75.5 MHz): δ 122.0 (*C*-5, SC_5H_4N), 124.8 (*C*-3, SC_5H_4N), 128.9 (*C*-3/*C*-5, C_6H_5), 131.4 (*C*-4, C_6H_5), 133.0 (*C*-2/*C*-6, C_6H_5), 142.9 (*C*-6, SC_5H_4N), 144.7 (*C*-4, SC_5H_4N), 161.2 (*C*-2, SC_5H_4N), (*C*-1, C_6H_5) not detected. ^{29}Si{^{1}H} NMR (99.4 MHz, −70 °C): δ −77.2. ^{15}N VACP/MAS NMR: δ −126.6. ^{29}Si VACP/MAS NMR: δ −76.5. Anal. Calcd for $C_{16}H_{13}IN_2S_2Si$ (452.41): C, 42.48; H, 2.90; N, 6.19; S, 14.18. Found: C, 42.2; H, 3.0; N, 6.3; S, 14.3.

Crystal Structure Analyses. Suitable single crystals of **4**−**6** and **8**−**12** were mounted in inert oil (perfluoropolyalkyl ether, ABCR) on a glass fiber and then transferred to the cold nitrogen gas stream of the diffractometer (Stoe IPDS diffractometer, graphite-monochromated Mo Kα radiation, λ = 0.71073 Å). All structures were solved by direct methods (*SHELXS-97*) and refined against all data by full-matrix least-squares methods on F^2 (*SHELXL-97*).[23] *SHELXLE*[24] was used as refinement GUI. The non-hydrogen atoms were refined anisotropically.[23] A riding model was employed in the refinement of the C*H* hydrogen atoms. The crystallographic data for the structures reported in this paper have been deposited with The Cambridge Crystallographic Data Centre as supplementary publications CCDC 948366−948373.

■ ASSOCIATED CONTENT

Supporting Information

Crystallographic data for compounds **4**−**6** and **8**−**12** (Tables S1 and S2), relative energies and bond lengths of selected species in the gas phase (Figures S1 and S2), Cartesian coordinates and total energies of selected species (Tables S3−S10), and CIF files giving the crystallographic data for **4**−**6** and **8**−**12**. This material is available free of charge via the Internet at http://pubs.acs.org.

■ AUTHOR INFORMATION

Corresponding Author

*E-mail: f.m.bickelhaupt@vu.nl (F.M.B.), r.tacke@uni-wuerzburg.de (R.T.). Phone: (+31)20-59-87617 (F.M.B.), (+49)931-31-85250 (R.T.). Fax: (+31)20-59-87629 (F.M.B.), (+49)931-31-84609 (R.T.).

Notes

The authors declare no competing financial interest.

■ ACKNOWLEDGMENTS

We thank the National Research School Combination—Catalysis (NRSC-C) and The Netherlands Organization for Scientific Research (NWO-CW and NWO-EW) for financial support. We thank the SARA supercomputer center in Amsterdam for excellent support.

■ REFERENCES

(1) (a) Junold, K.; Burschka, C.; Bertermann, R.; Tacke, R. *Dalton Trans.* **2010**, *39*, 9401−9413. (b) Junold, K.; Baus, J. A.; Burschka, C.; Tacke, R. *Angew. Chem.* **2012**, *124*, 7126−7129; *Angew. Chem., Int. Ed.* **2012**, *51*, 7020−7023.

(2) Selected publications dealing with higher-coordinate silicon(IV) complexes with sulfur ligand atoms: (a) Tacke, R.; Mallak, M.; Willeke, R. *Angew. Chem.* **2001**, *113*, 2401−2403; *Angew. Chem., Int. Ed.* **2001**, *40*, 2339−2341. (b) Naganuma, K.; Kawashima, T. *J. Organomet. Chem.* **2002**, *643*−*644*, 504−507. (c) Bertermann, R.; Biller, A.; Kaupp, M.; Penka, M.; Seiler, O.; Tacke, R. *Organometallics* **2003**, *22*, 4104−4110. (d) Troegel, D.; Burschka, C.; Riedel, S.; Kaupp, M.; Tacke, R. *Angew. Chem.* **2007**, *119*, 7131−7135; *Angew. Chem., Int. Ed.* **2007**, *46*, 7001−7005. (e) Metz, S.; Burschka, C.; Platte, D.; Tacke, R. *Angew. Chem.* **2007**, *119*, 7136−7139; *Angew. Chem., Int. Ed.* **2007**, *46*, 7006−7009. (f) So, C.-W.; Roesky, H. W.; Oswald, R. B.; Pal, A.; Jones, P. G. *Dalton Trans.* **2007**, 5241−5244. (g) Metz, S.; Burschka, C.; Tacke, R. *Eur. J. Inorg. Chem.* **2008**, 4433−4439. (h) Metz, S.; Burschka, C.; Tacke, R. *Organometallics* **2009**, *28*, 2311−2317. (i) Theis, B.; Metz, S.; Burschka, C.; Bertermann, R.; Maisch, S.; Tacke, R. *Chem.—Eur. J.* **2009**, *15*, 7329−7338. (j) See ref 1a. (k) Wagler, J.; Brendler, E.; Langer, T.; Pöttgen, R.; Heine, T.; Zhechkov, L. *Chem.—Eur. J.* **2010**, *16*, 13429−13434. (l) Metz, S.; Theis, B.; Burschka, C.; Tacke, R. *Chem.—Eur. J.* **2010**, *16*, 6844−6856. (m) Kobelt, C.; Burschka, C.; Bertermann, R.; Fonseca Guerra, C.; Bickelhaupt, F. M.; Tacke, R. *Dalton Trans.* **2012**, *41*, 2148−2162. (n) Junold, K.; Baus, J. A.; Burschka, C.; Auerhammer, D.; Tacke, R. *Chem.—Eur. J.* **2012**, *18*, 16288−16291.

(3) Selected publications dealing with higher-coordinate silicon(IV) complexes with pyridine-type ligands: (a) Wannagat, U.; Hensen, K.; Petesch, P.; Vielberg, F. *Monatsh. Chem.* **1967**, *98*, 1415−1422. (b) Kummer, D.; Köster, H. *Angew. Chem.* **1969**, *81*, 897−898; *Angew. Chem., Int. Ed. Engl.* **1969**, *8*, 878−879. (c) Kummer, D.; Balkir, A.; Köster, H. *J. Organomet. Chem.* **1979**, *178*, 29−54. (d) Kummer, D.; Chaudhry, S. C.; Debaerdemaeker, T.; Thewalt, U. *Chem. Ber.* **1990**, *123*, 945−951. (e) Kummer, D.; Chaudhry, S. C.; Depmeier, W.; Mattern, G. *Chem. Ber.* **1990**, *123*, 2241−2245. (f) Fleischer, H.; Hensen, K.; Stumpf, T. *Chem. Ber.* **1996**, *129*, 765−771. (g) Hensen, K.; Stumpf, T.; Bolte, M.; Näther, C.; Fleischer, H. *J. Am. Chem. Soc.* **1998**, *120*, 10402−10408. (h) Hensen, K.; Mayr-Stein, R.; Spangenberg, B.; Bolte, M.; Rühl, S. *Z. Naturforsch.* **2000**, *55b*, 248−252. (i) Hensen, K.; Kettner, M.; Stumpf, T.; Bolte, M. *Z. Naturforsch.* **2000**, *55b*, 901−906. (j) van den Ancker, T. R.; Raston, C. L.; Skelton, B. W.; White, A. H. *Organometallics* **2000**, *19*, 4437−4444. (k) Jones, C.; Junk, P. C.; Leary, S. G.; Smithies, N. A.; Steed, J. W. *Inorg. Chem. Commun.* **2002**, *5*, 533−536. (l) Nakash, M.; Gut, D.; Goldvaser, M. *Inorg. Chem.* **2005**, *44*, 1023−1030. (m) Wagler, J.; Schley, M.; Gerlach, D.; Böhme, U.; Brendler, E.; Roewer, G. *Z. Naturforsch.* **2005**, *60b*, 1054−1064. (n) Wagler, J.; Gerlach, D.; Roewer, G. *Chem. Heterocycl. Compd.* **2006**, *42*, 1557−1567. (o) Brendler, E.; Wächtler, E.; Wagler, J. *Organometallics* **2009**, *28*, 5459−5465. (p) Fester, G. W.; Wagler, J.; Brendler, E.; Böhme, U.; Gerlach, D.; Kroke, E. *J. Am. Chem. Soc.* **2009**, *131*, 6855−6864. (q) Portius, P.; Davis, M. *Dalton Trans.* **2010**, *39*, 527−532. (r) Portius, P.; Filippou, A. C.; Schnakenburg, G.; Davis, M.; Wehrstedt, K.-D. *Angew. Chem.* **2010**,

122, 8185−8189; *Angew. Chem., Int. Ed.* **2010**, *49*, 8013−8016. (s) Fester, G. W.; Eckstein, J.; Gerlach, D.; Wagler, J.; Brendler, E.; Kroke, E. *Inorg. Chem.* **2010**, *49*, 2667−2673. (t) Junold, K.; Burschka, C.; Bertermann, R.; Tacke, R. *Dalton Trans.* **2011**, *40*, 9844−9857. (u) See ref 2k.

(4) Selected transition-metal complexes with the *N*,*S*-pyridine-2-thiolato(−) ligand: (a) Fletcher, S. R.; Skapski, A. C. *J. Chem. Soc., Dalton Trans.* **1972**, 635−639. (b) Evans, I. P.; Wilkinson, G. *J. Chem. Soc., Dalton Trans.* **1974**, 946−951. (c) Mura, P.; Olby, B. G.; Robinson, S. D. *J. Chem. Soc., Dalton Trans.* **1985**, 2101−2112. (d) Zhang, N.; Wilson, S. R.; Shapley, P. A. *Organometallics* **1988**, *7*, 1126−1131. (e) Umakoshi, K.; Ichimura, A.; Kinoshita, I.; Ooi, S. *Inorg. Chem.* **1990**, *29*, 4005−4010. (f) Reynolds, J. G.; Sendlinger, S. C.; Murray, A. M.; Huffman, J. C.; Christou, G. *Inorg. Chem.* **1995**, *34*, 5745−5752. (g) Su, W.; Hong, M.; Weng, J.; Cao, R.; Lu, S. *Angew. Chem.* **2000**, *112*, 3033−3036; *Angew. Chem., Int. Ed.* **2000**, *39*, 2911−2914. (h) Liaw, W.-F.; Lee, J.-H.; Gau, H.-B.; Chen, C.-H.; Jung, S.-J.; Hung, C.-H.; Chen, W.-Y.; Hu, C.-H.; Lee, G.-H. *J. Am. Chem. Soc.* **2002**, *124*, 1680−1688. (i) Halder, P.; Paine, T. K. *Inorg. Chem.* **2011**, *50*, 708−710.

(5) Group 1 and 2 element complexes with ligands of the *N*,*S*-pyridine-2-thiolato(−) type: (a) Chadwick, S.; Ruhlandt-Senge, K. *Chem.—Eur. J.* **1998**, *4*, 1768−1780. (b) Chadwick, S.; Englich, U.; Senge, M. O.; Noll, B. C.; Ruhlandt-Senge, K. *Organometallics* **1998**, *17*, 3077−3086. (c) Sousa Pedrares, A.; Teng, W.; Ruhlandt-Senge, K. *Chem.—Eur. J.* **2003**, *9*, 2019−2024.

(6) Group 13 element complexes with ligands of the *N*,*S*-pyridine-2-thiolato(−) type: (a) Castaño, M. V.; Sánchez, A.; Casas, J. S.; Sordo, J.; Briansó, J. L.; Piniella, J. F.; Solans, X.; Germain, G.; Debaerdemaeker, T.; Glaser, J. *Organometallics* **1988**, *7*, 1897−1904. (b) Rose, D. J.; Chang, Y. D.; Chen, Q.; Kettler, P. B.; Zubieta, J. *Inorg. Chem.* **1995**, *34*, 3973−3979. (c) Landry, C. C.; Hynes, A.; Barron, A. R.; Haiduc, I.; Silvestru, C. *Polyhedron* **1996**, *15*, 391−402. (d) Abram, S.; Maichle-Mössmer, C.; Abram, U. *Polyhedron* **1997**, *16*, 2291−2298.

(7) Group 14 element complexes with ligands of the *N*,*S*-pyridine-2-thiolato(−) type: (a) Masaki, M.; Matsunami, S. *Bull. Chem. Soc. Jpn.* **1976**, *49*, 3274−3279. (b) Damude, L. C.; Dean, P. A. W.; Manivannan, V.; Srivastava, R. S.; Vittal, J. J. *Can. J. Chem.* **1990**, *68*, 1323−1331. (c) Block, E.; Ofori-Okai, G.; Kang, H.; Wu, J.; Zubieta, J. *Inorg. Chim. Acta* **1991**, *190*, 5−6. (d) Schmiedgen, R.; Huber, F.; Preut, H.; Ruisi, G.; Barbieri, R. *Appl. Organomet. Chem.* **1994**, *8*, 397−407. (e) Couce, M. D.; Faraglia, G.; Russo, U.; Sindellari, L.; Valle, G. *J. Organomet. Chem.* **1996**, *513*, 77−83. (f) Couce, M. D.; Cherchi, V.; Faraglia, G.; Russo, U.; Sindellari, L.; Valle, G.; Zancan, N. *Appl. Organomet. Chem.* **1996**, *10*, 35−45. (g) Huber, F.; Schmiedgen, R.; Schürmann, M.; Barbieri, R.; Ruisi, G.; Silvestri, A. *Appl. Organomet. Chem.* **1997**, *11*, 869−888. (h) Sousa-Pedrares, A.; Casanova, M. I.; García-Vázquez, J. A.; Durán, M. L.; Romero, J.; Sousa, A.; Silver, J.; Titler, P. J. *Eur. J. Inorg. Chem.* **2003**, 678−686. (i) Ma, C.; Jiang, Q.; Zhang, R. *Can. J. Chem.* **2004**, *82*, 608−615. (j) Xanthopoulou, M. N.; Hadjikakou, S. K.; Hadjiliadis, N.; Kubicki, M.; Karkabounas, S.; Charalabopoulos, K.; Kourkoumelis, N.; Bakas, T. *J. Organomet. Chem.* **2006**, *691*, 1780−1789.

(8) Group 15 element complexes with ligands of the *N*,*S*-pyridine-2-thiolato(−) type: (a) Preut, H.; Huber, F.; Hengstmann, K.-H. *Acta Crystallogr., Sect. C* **1988**, *44*, 468−469. (b) Kennepohl, D. K.; Pinkerton, A. A.; Lee, Y. F.; Cavell, R. G. *Inorg. Chem.* **1990**, *29*, 5088−5096. (c) Hengstmann, K.-H.; Huber, F.; Preut, H. *Acta Crystallogr., Sect. C* **1991**, *47*, 2029−2032. (d) Block, E.; Ofori-Okai, G.; Kang, H.; Wu, J.; Zubieta, J. *Inorg. Chem.* **1991**, *30*, 4784−4788.

(9) Selected reviews dealing with higher-coordinate silicon(IV) compounds: (a) Holmes, R. R. *Chem. Rev.* **1996**, *96*, 927−950. (b) Pestunovich, V.; Kirpichenko, S.; Voronkov, M. In *The Chemistry of Organic Silicon Compounds*; Rappoport, Z., Apeloig, Y., Eds.; Wiley: Chichester, U.K., 1998; Vol. 2, Part 2, pp 1447−1537. (c) Chuit, C.; Corriu, R. J. P.; Reye, C. In *Chemistry of Hypervalent Compounds*; Akiba, K.-y., Ed.; Wiley-VCH: New York, 1999; pp 81−146. (d) Tacke, R.; Pülm, M.; Wagner, B. *Adv. Organomet. Chem.* **1999**, *44*, 221−273. (e) Brook, M. A. *Silicon in Organic, Organometallic and Polymer Chemistry*; Wiley: New York, 2000; pp 97−114. (f) Tacke, R.; Seiler, O. In *Silicon Chemistry: From the Atom to Extended Systems*; Jutzi, P., Schubert, U., Eds.; Wiley-VCH: Weinheim, Germany, 2003; pp 324−337. (g) Kost, D.; Kalikhman, I. *Adv. Organomet. Chem.* **2004**, *50*, 1−106. (h) Voronkov, M. G.; Trofimova, O. M.; Bolgova, Y. I.; Chernov, N. F. *Russ. Chem. Rev.* **2007**, *76*, 825−845. (i) Kost, D.; Kalikhman, I. *Acc. Chem. Res.* **2009**, *42*, 303−314. (j) Couzijn, E. P. A.; Slootweg, J. C.; Ehlers, A. W.; Lammertsma, K. *Z. Anorg. Allg. Chem.* **2009**, *635*, 1273−1278.

(10) The Berry distortion was analyzed by using the *PLATON* program system: Spek, A. L. *Acta Crystallogr., Sect. D* **2009**, *65*, 148−155.

(11) Because of a poor signal-to-noise ratio (despite a long measurement time), analysis of the solid-state ^{15}N NMR spectrum was very difficult.

(12) Böhm, J.; Fenzke, D.; Pfeifer, H. *J. Magn. Reson.* **1983**, *55*, 197−204.

(13) (a) te Velde, G.; Bickelhaupt, F. M.; Baerends, E. J.; Fonseca Guerra, C.; van Gisbergen, S. J. A.; Snijders, J. G.; Ziegler, T. *J. Comput. Chem.* **2001**, *22*, 931−967. (b) http://www.scm.com.

(14) (a) Vosko, S. H.; Wilk, L.; Nusair, M. *Can. J. Phys.* **1980**, *58*, 1200−1211. (b) Becke, A. D. *Phys. Rev. A* **1988**, *38*, 3098−3100. (c) Perdew, J. P. *Phys. Rev. B* **1986**, *33*, 8822−8824; Erratum: *Phys. Rev. B* **1986**, *34*, 7406.

(15) (a) van Lenthe, E.; Baerends, E. J.; Snijders, J. G. *J. Chem. Phys.* **1994**, *101*, 9783−9792. (b) van Lenthe, E.; van Leeuwen, R.; Baerends, E. J.; Snijders, J. G. *Int. J. Quantum Chem.* **1996**, *57*, 281−293.

(16) (a) Klamt, A.; Schüürmann, G. *J. Chem. Soc., Perkin Trans. 2* **1993**, 799−805. (b) Klamt, A. *J. Phys. Chem.* **1995**, *99*, 2224−2235. (c) Pye, C. C.; Ziegler, T. *Theor. Chem. Acc.* **1999**, *101*, 396−408. (d) Swart, M.; Rösler, E.; Bickelhaupt, F. M. *Eur. J. Inorg. Chem.* **2007**, 3646−3654.

(17) (a) Bickelhaupt, F. M.; Baerends, E. J. In *Reviews in Computational Chemistry*; Lipkowitz, K. B., Boyd, D. B., Eds.; Wiley-VCH: New York, 2000; Vol. *15*, pp 1−86. (b) Bickelhaupt, F. M.; Diefenbach, A.; de Visser, S. P.; de Koning, L. J.; Nibbering, N. M. M. *J. Phys. Chem. A* **1998**, *102*, 9549−9553.

(18) (a) Bickelhaupt, F. M.; van Eikema Hommes, N. J. R.; Fonseca Guerra, C.; Baerends, E. J. *Organometallics* **1996**, *15*, 2923−2931. (b) Fonseca Guerra, C.; Handgraaf, J.-W.; Baerends, E. J.; Bickelhaupt, F. M. *J. Comput. Chem.* **2004**, *25*, 189−210.

(19) (a) Swart, M.; Bickelhaupt, F. M. *J. Chem. Theory Comput.* **2006**, *2*, 281−287. (b) See ref 14. (c) van Zeist, W.-J.; Ren, Y.; Bickelhaupt, F. M. *Sci. China Chem.* **2010**, *53*, 210−215.

(20) (a) Mulder, R. J.; Fonseca Guerra, C.; Bickelhaupt, F. M. *J. Phys. Chem. A* **2010**, *114*, 7604−7608. (b) Ruiz, J. M.; Mulder, R. J.; Fonseca Guerra, C.; Bickelhaupt, F. M. *J. Comput. Chem.* **2011**, *32*, 681−688.

(21) (a) Bento, A. P.; Bickelhaupt, F. M. *J. Org. Chem.* **2008**, *73*, 7290−7299. (b) Pierrefixe, S. C. A. H.; van Stralen, S. J. M.; van Stralen, J. N. P.; Fonseca Guerra, C.; Bickelhaupt, F. M. *Angew. Chem.* **2009**, *121*, 6591−6593; *Angew. Chem., Int. Ed.* **2009**, *48*, 6469−6471.

(22) Berger, S.; Braun, S. *200 and More NMR Experiments: A Practical Course*; VCH: Weinheim, Germany, 2004; pp 141−144.

(23) Sheldrick, G. M. *Acta Crystallogr., Sect. A* **2008**, *64*, 112−122.

(24) Hübschle, C. B.; Sheldrick, G. M.; Dittrich, B. *J. Appl. Crystallogr.* **2011**, *44*, 1281−1284.